Synthesis of Reductive Nanogels Cross-linked with Polyanions to Mimic Oligonucleotides

Yuanfeng Wang

A Thesis in the Department of Chemistry & Biochemistry

Presented in Partial Fulfillment of the Requirements
For the Degree of Master of Science (Chemistry)
At Concordia University
Montreal, Quebec, Canada

September 2023

CONCORDIA UNIVERSITY
School of Graduate Studies

This is to certify that the thesis prepared

By: Yuanfeng Wang

Entitled: Synthesis of Reductive Nanogels Cross-linked with Polyanions to Mimic Oligonuceotides

and submitted in partial fulfillment of the requirements for the degree of

Master of Science (Chemistry)

complies with the regulations of the University and meets the accepted standards with respect to originality and quality.

Signed by the final Examining Committee:

_____ Chair

Dr. Cameron Skinner

_____ Examiner

Dr. Marek B. Majewski

_____ Examiner

Dr. Zhibin Ye

_____ Supervisor

Dr. John Oh & Dr. Christopher Wilds

Approved by _____

Dr. Louis Cuccia, Graduate Program Director

September 15th, 2023 _____

Dr. Pascale Sicotte, Dean of Faculty

Abstract

Synthesis of Reductive Nanogels Cross-linked with Polyanions to Mimic Oligonuceotides

Yuanfeng Wang

Gene therapy with nucleic acid-based therapeutic agents has emerged as a promising strategy to treat various human diseases. However, the efficient delivery of nucleic acids faces a critical challenge as they are susceptible to hydrolytic and enzymatic degradation during blood circulation and in the body. The conventional delivery strategy for nucleic acids involves cationic polymers which bind with the anionic phosphate groups of the nucleic acid by ionic interaction to form polyplexes. These polyplexes are designed for effective endosomal escape of the nucleic acids through the proton-sponge effect, leading to release of their cargos, resulting in excellent gene transfection. However, the polyplex-based nanocarriers present critical drawbacks including cytotoxicity of cationic polymers, the degradation of nucleic acids in polyplexes, and the propensity to aggregate with serum proteins during blood circulation.

My MSc thesis focuses on the exploration of a new paradigm for nucleic acid delivery which explores the design of reactive, but neutral hydrophilic copolymers and the use of nucleic acids as therapeutics and cross-linkers. A poly(phosphonic acid) with terminal thiol groups to mimic oligonucleotides is synthesized by reversible addition fragmentation chain-transfer polymerization. Consequently, the poly(phosphonic acid) is covalently conjugated with a water-soluble random copolymer bearing pendant pyridyl-disulfide functional groups through a thiol-disulfide exchange reaction in aqueous solution, resulting in the formation of cross-linked nanogels through the formation of new disulfide bonds. Consequently, the reductive cleavage of the disulfide linkages in the fabricated nanogels has the potential to prompt the detachment of therapeutic nucleic acids from the nanogel cores. The enhanced release of nucleic acids through degradation (or destabilization) of nanogel cores can occur in the presence of glutathione inside cells.

Acknowledgments

This project was supervised by Dr. John Oh and Dr. Christopher Wilds. I would like to acknowledge and give my warmest thanks to them for their patient guidance and support through all the stages of my project. I also thank my supervisory committee members, Dr. Zhibin Ye and Dr. Marek Majewski and academic co-supervisor Dr. Matt Moffitt at the Department of Chemistry at the University of Victoria.

I greatly acknowledge FRQNT Team Grant, NSERC CREATE entitled "Polymer Nanoparticles for Drug Delivery (PoND)" and Concordia University for their financial supports to my M.Sc. studies. In addition, I would like to thank all Dr. Oh and Dr. Wilds' lab members as they helped me a lot during my entire study and research progress, especially to Dr. Pothana Gandhi and Xiaolei Hu for their efforts and time to teach polymer science as well as the lab techniques.

I would also like to give special thanks to my girlfriend (Linyi) and my family as a whole for their continuous support and understanding.

Contribution of Authors

Most of the experiments were carried by myself under the guidance of Professors Oh and Wilds, except for the synthesis and structural characterization of EG-RAFT (a difunctional RAFT agent) by Xiaolei Hu (a former MSc student in the Professor Oh's laboratory) and DEPMMA by Dr. Pothana Gandhi Nellepalli (a former postdoctoral fellow in the Professor Oh's laboratory).

Table of Contents

List of Figures

List of Tables

List of Symbols and Abbreviations

AIBN	Azobisisobutyronitrile
ATRP	Atom Transfer Radical Polymerization
CTA	Chain Transfer Agent
DCM	Dichloromethane
DEPMMA	Diethoxyphosphoryl Methyl Methacrylate
DLS	Dynamic Light Scattering
DMF	Dimethylformamide
DMSO	Dimethyl Sulfoxide
DNA	Deoxyribonucleic Acid
DTNB	5,5'-dithio-bis-(2-nitrobenzoic acid)
DOX	Doxorubicin
EDC	1-Ethyl-3-(3-dimethylaminopropyl)carbodiimide
GPC	Gel Permeation Chromatography
LCST	Lower Critical Solution Temperature
MMA	Methyl Methacrylate
NMR	Nuclear Magnetic Resonance
NPs	Nanoparticles
NTB	2-Nitro-5-thiobenzoic Acid
OEOMA	Oligo(ethylene oxide) Monomethyl Ether Methacrylate
PBS	Phosphate Buffer Saline
PDSEMA	Pyridyldisulfide Ethylmethacrylate
PEG	Polyethylene Glycol
PEO	Poly(ethylene oxide)
PPA	Poly(phosphonic acid)
RAFT	Reversible Addition Fragmentation Chain-transfer

RNA	Ribonucleic Acid
TEA	Triethylamine
THF	Tetrahydrofuran
UV/Vis	Ultraviolet/Visible

Chapter 1 Introduction

1.1 Composition of Nucleic Acids

Nucleic acids are macromolecules consisting of nucleotide building blocks. Their typical types that occur naturally include deoxyribonucleic acid (DNA) and ribonucleic acid (RNA). DNA was first identified in the late 1860s by Friedrich Miescher [1]. Following Miescher's discovery, other scientists figured out additional details about the DNA molecule, including its primary chemical components and the ways in which they joined with one another [2]. On 1953, Watson and Crick concluded that the DNA molecule exists in the form of a three-dimensional double helix with the two strands connected by hydrogen bonds. The DNA double helix is anti-parallel, which means that the 5' end of one strand is paired with the 3' end of its complementary strand [3-6].

DNA is a polymer made of monomeric units called nucleotides as shown in Figure 1.1. A nucleotide is composed of a 5-carbon sugar, 2'-deoxyribose, a nitrogenous base and one or more phosphate groups. A DNA strand containing four nucleotides with the nitrogenous bases thymine (T), cytosine (C), adenine (A) and guanine (G) respectively. The 3′ carbon of one nucleotide is linked to the 5′ carbon of the next via a phosphodiester group. DNA is the genetic material that can replicate or generate duplicates of itself which able the new cells include an identical replica of the DNA that found in the old one when cells divide [7].

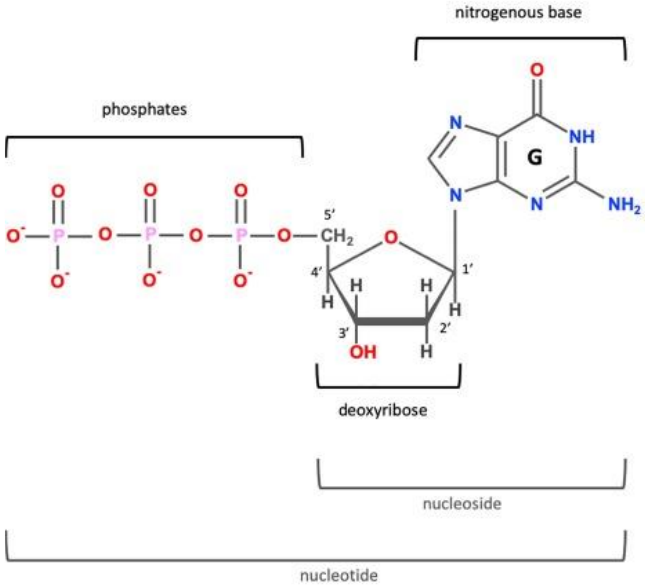

Figure 1.1. Structure of a DNA nucleoside and nucleotide [7].

RNA can convert the genetic code into protein to carry out cellular functions. RNA has some chemical difference relative to DNA. The nucleotide of RNA contains a 5-carbon sugar ribose, a phosphate and a nitrogenous base. The phosphate is attached to the 5′ carbon of the ribose and the nitrogenous base to the 1′ carbon. RNA contains four bases adenine, guanine, cytosine, and uracil. Both DNA and RNA are polyanionic as they are polymers of nucleotides with alternating sugars and negatively charged phosphate groups in the backbone [7].

1.2 Therapeutic Applications of Nucleic Acids

1.2.1 Nucleic acid based therapeutics

Nucleic acid-based therapies (called gene therapy) have emerged as attractive approaches to treat a variety of human diseases [8]. Various forms of nucleic acid-based therapeutics have been used to selectively act on proteins, transcripts, and genes that cannot be targeted by conventional small molecules or proteins. Although various types of nucleic acid-based therapies exist, they share a common mechanism of action based on sequence-specific recognition of endogenous nucleic acids mediated by Watson-Crick base pairing [9-12].

In the past decades, several nucleic acid therapeutics have been approved and developed, such as antisense oligonucleotides (ASOs), RNA interference (RNAi), splice-switching oligonucleotides (SSOs) etc. [13] ASOs is a single stranded oligonucleotide that pairs with a complementary region on an RNA via Watson–Crick H-bonds and then acts, for example, via a steric block, splice site shifting or RNase-H mediated RNA degradation mechanism [14]. RNAi is a promising therapeutic strategy mediated by small interfering RNA (siRNA), which consists of synthetic RNA double-stranded bodies designed to specifically target specific messenger RNA (mRNA) for degradation [15]. Effective siRNA delivery leads to highly specific knockdown of genes, which reduce protein target expression effectively. However, this and other recent genetic applications require successful and efficient transport of nucleic acids into target tissues and organs to regulate gene expression. Meanwhile, natural or synthetic nucleic acids are susceptible to hydrolysis and enzymatic degradation during blood circulation and in vivo. Therefore, efficient delivery of nucleic acids that avoid enzymatic degradation in serum remains as the big challenge for the success of nucleic acid-based therapies [16].

A conventional delivery strategy that has been widely explored is the development of non-viral carriers based on positively charged (or cationic) polymers that form complexes by ion complexation with negatively charged nucleic acid phosphate groups [17]. Upon reaching the target tissue, the nucleic acid can be released from the intracellular complex, subsequently escaping from the intranuclear body and finally transferring to the nucleus. Thus, most complexes are carefully designed to efficiently escape nucleic acids from endosomes through the so-called proton sponge (or pH buffering) effect, resulting in excellent gene transfection [18].

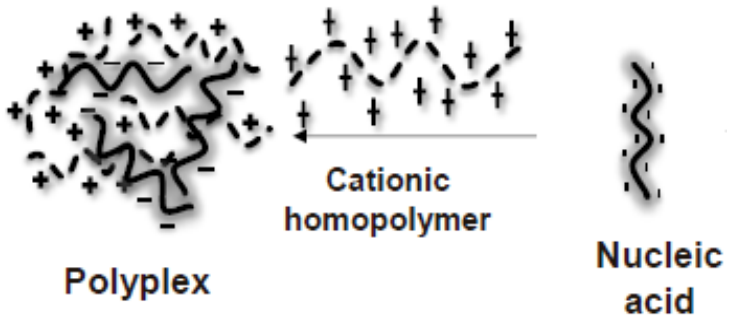

Figure 1.2. Schematic illustration of conventional polyplex model for delivery of nucleic acids. Courtesy of Professor. Oh.

1.2.2. Endosomal escape for gene transfection in polyplex model

Complexes modified with ligand molecules are actively internalized by specific binding to cell surface receptors (receptor-mediated endocytosis), which is considered as a more efficient method for targeted gene delivery. Because endocytosed substances are destined to be localized in digesting organelles, lysosomes, the endosomal escape function of the complexes should be the key to high transfection efficiency [19]. Endosomal sorting of nanoparticles is described in detail in the following paragraphs. A great number of endocytosed nanoparticles are first delivered to a focal point for endosomal sorting, called early endosomes. The luminal pH of the early endosome is approximately

6.2-6.8 [20], significantly lower than the extracellular pH of 7.4. Once in the early endosome, most nanoparticles are transported to the pre-lysosomal compartment, called the late endosome, and then enter the lysosomal degradation pathway. In detail, nanoparticle sorting from the early endosome to the late endosome typically begins with acidification of the early endosomal lumen, followed by movement from the cell periphery to the perinuclear region on the microtubule track. The luminal pH in late endosomes is approximately 5.0-5.5, which differs from that in the early endosomal and extracellular environments. This decrease from a neutral extracellular pH to an acidic pH in late endosomes may be important for the endosomal escape function of viral and nonviral vectors. Indeed, some viral proteins, such as the pentamer in adenovirus and hemagglutinin in influenza virus, undergo structural changes and become hydrophobic due to the decrease in pH [21]. As a result, these proteins can interact more strongly with the endosomal membrane, leading to virion escape from the endosome by disruption or fusion.

1.2.3 Examples and properties of cationic polymers

Cationic polymers having primary, secondary, and tertiary amine groups can form complexes with nucleic acids through electrostatic interactions (entitled polyplexes). Figure 1.4 shows some exemples of common cationic polymers including polyethyleneimine (PEI), poly(L-lysine) (PLL), and poly(N,N-dimethylaminoethyl methacrylate) (PDMAEMA). These polymers have been extensively explored for the fabrication of polyplexes to transfer nucleic acids into the interior of cells [22,23].

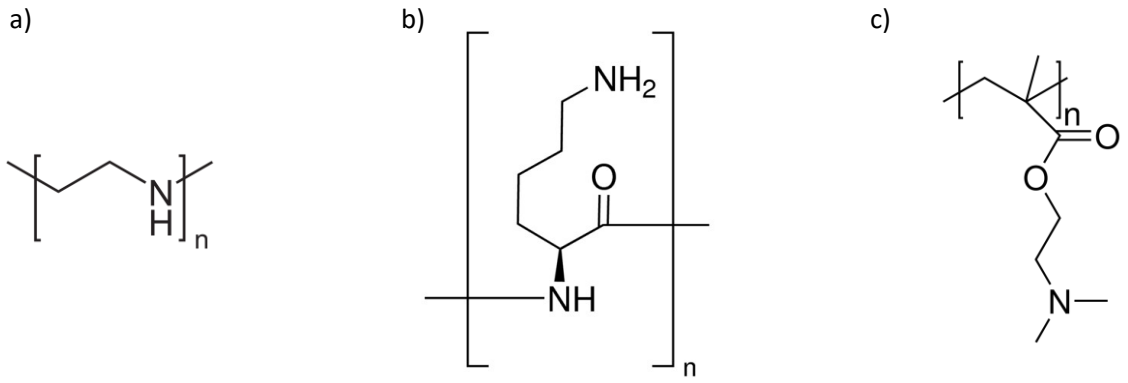

Figure 1.3. Chemical structures of typical cationic polymers explored for nucleic acid. delivery including a) PEI, b) PLL, and c) PDMAEMA.

One of the first cationic polymers explored for nucleic acid delivery was PLL as it has high cationic charge density necessary for DNA condensation [24]. However, since it could not transfect cells on its own, it was soon realized that other compounds needed to be added to induce endosomal release (e.g., chloroquine or fusion peptides that cause endosomal disruption) [25]. It was discovered that several cationic polymers with significant buffering capacity below physiological pH (e.g., lipopolysamines and polyamideamines) could achieve high transfection efficiency without the addition of such membrane-disrupting agents [26].

This observation led to investigation of the gene delivery potential of PEI, a synthetic cationic polymer with high amine density and high buffering capacity [27]. PEI can complex with negatively-charged nucleic acids or protein antigens to form small particles amenable to cellular uptake. PEI-based polyplex in the endosomes can induce the influx of protons and their counter ions, thereby causing osmotic swelling and rupture of endosome and helping the complex to escape the endosome, called the proton-sponge effect [28].

PDMAEMA is an interesting vector for the design of a gene transfection system as it contains only tertiary amines and reaches 90 % of the transfection efficiency of PEI. The PDMAEMAs

with a molecular weight > 112 kDa are more efficient in transfection but at the expense of toxicity [29]. Cytotoxicity can be reduced by designing lower molecular weight cationic polymers. Therefore, an optimum molecular weight showing acceptable efficiency and toxicity was required. Recently this parameter was established by making different molecular weight PDMAEMAs by controlled radical polymerization and shown it to be about 60 kDa [30].

1.2.4 Challenges of polyplex-based gene delivery strategy

Polyplex-based therapeutic nucleic acid nanocarriers have key drawbacks that must be addressed. One drawback is cytotoxicity. Cationic polymers are known to be highly toxic to cells. Some studies have shown that cytotoxicity can be reduced by designing shorter chain cationic polymers, for example PEI. However, complexes formed with shorter PEI chains exhibit reduced gene transfection [31]. A second disadvantage is the degradation of nucleic acids in the complexes. Polymerization utilizes ionic interactions between cationic polymers and nucleic acids. Such ionic complexes (amine-phosphate complexes) can be exposed to serum proteins during blood circulation, leading to degradation of the complexes and nucleic acids [32]. A third disadvantage is the tendency to form aggregate with serum proteins during circulation. Most of the reported complexes usually have Zeta potentials > 10 mV, which may be due to the presence of free cationic groups in the complexes. These cations can interact with serum proteins during circulation, leading to unwanted aggregation in the blood [33]. These drawbacks are mainly attributed to the ionic complexation of the cationic polymer with negatively charged nucleic acids.

1.3 Stimuli-responsive degradation

Stimuli-responsive degradation (SRD) has been significantly explored as a promising platform in the development of smart/degradable materials for biological and biomedical applications [34-36]. SRD involves the incorporation of labile bonds into the design of polymeric materials, and they are degraded

through chemical transition upon the cleavage of the labile bonds in response to external stimuli. Acidic pH, light, and glucose as well as reductive, oxidative, and enzymatic reactions have been extensively explored as stimuli (or triggers) for the development of smart nanomaterials [37-42].

In particular, disulfide bonds (-SS-) are unique in that they can be cleaved in a reducing environment (or in the presence of reducing agent) to corresponding thiols, which can be oxidized to reform the corresponding disulfide bonds [43]. Glutathione (GSH) is a tripeptide consisting of a cystine residue (bearing pendant SH group). GSH is found in millimolar concentration in an intracellular compartment (0.1-10 mM). While its concentration is <10 μM in an extracellular compartment and bloods, it is known to be 4-5 times greater in cancer cells and tumor tissues, compared with normal cells and tissues [44].

Due to these features, disulfide-based degradable chemistry has been extensively explored in the development of gene delivery nanocarriers. A report describes the synthesis of a cationic diblock copolymer consisting of a hydrophobic polylactide (PLA) block and a cationic PDMAEMA block. Both blocks are covalently linked with reductively cleavable disulfide bonds. The synthesized PLA-ss-PDMAEMA block copolymer self-assembled to form nanoassemblies with PLA cores surrounded with PDMAEMA corona. The hydrophobic core can encapsulate DOX drugs and the cationic corona enabled the formation of complex with nucleic acids, thus forming core/shell-type polyplexes. The cleavage of disulfide bonds at the interfaces of core/corona allowed for the enhanced release of both DOX drugs and nucleic acids. In absence of GSH, the encapsulated DOX is presumably confined in small micellar cores as shown in Figure 1.5. In the presence of 10 mM GSH, DOX-loaded copolymer degraded and enabled the enhanced release of DOX to aqueous solution as shown in Figure 1.5 [45].

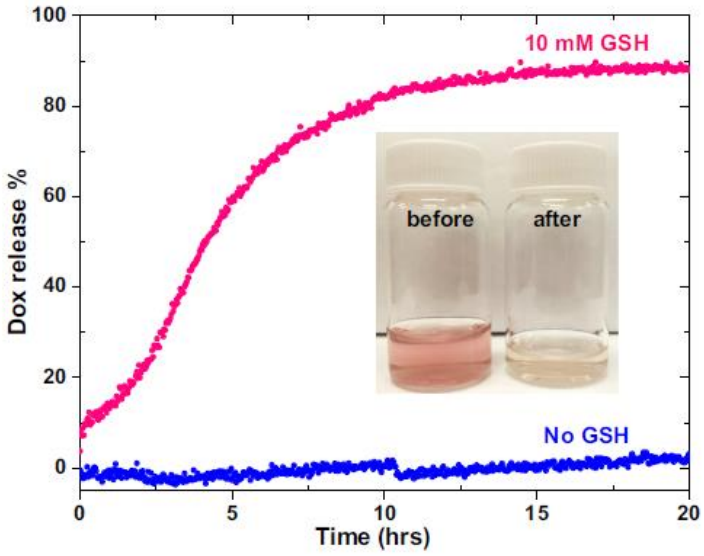

Figure 1.4. Scheme for release of DOX from DOX-loaded micelles in 10 mM aqueous GSH solution buffered with PBS, and aqueous PBS as a control [45].

Another report describes the synthesis of poly(ethylene glycol) (PEG)-based cationic block copolymer with a cationic block of a random copolymer consisting of DMAEMA and a methacrylate bearing pendant disulfide bond (called HmssEt). Both blocks are connected with an acid-labile acetal (Ac) linkage, thus forming PEG-Ac-P(DMAEMA-co-HmssEt) as shown in Figure 1.6. The synthesized block copolymer formed micelleplexes consisting of P(DMAEMA-co-HmssEt) cores that are complexed with nucleic acids, which are surrounded with PEG corona. The cleavage of pendant disulfide linkages in the presence of GSH enhanced the release of nucleic acids [46].

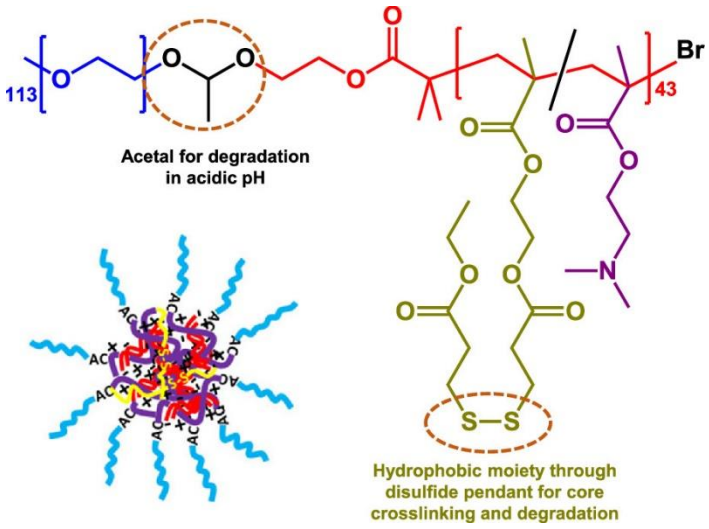

Figure 1.5. Scheme of a dual-location dual-acid/glutathione-responsive degradable block copolymer [46].

Despite these advances, most disulfide-bearing gene delivery nanocarriers exhibiting enhanced release of nucleic acids have been designed for gene encapsulation through ionic interactions of cationic polymer blocks with nucleic acids.

1.4 Thermoresponsive polymers

Polymers that are responsive to change in temperature are known to be thermoresponsive polymers that have been employed in various areas such as drug delivery, gene delivery and tissue engineering. There are two main types of thermosensitive polymers; the first type exhibits a lower critical solution temperature (called LCST), while the second type exhibits an upper critical solution temperature (called UCST) [47].

Both LCST and UCST are the respective critical temperature points below and above which the polymer and solvent are completely miscible. For example, a polymer solution at temperatures below LCST is clear and homogeneous, while the polymer solution at temperatures at above LCST appears

cloudy (resulting in the LCST also known as the cloudiness point) [48-50]. Such change happens because it is more energetically favorable. In particular, using the Gibbs equation $\Delta G = \Delta H - T\Delta S$ (G: Gibbs free energy, H: enthalpy and S: entropy) to consider the free energy of the system, the reason why phase separation is more favorable at increasing temperatures is mainly due to the entropy of the system. Specifically, the main driving force is the entropy of the water, which is less ordered and higher when the polymer is not in solution. This is also known as the "hydrophobic effect". It is worth noting that LCST is an entropy-driven effect, while UCST is an enthalpy-driven effect [51,52].

A typical thermoresponsive polymer exhibiting LCST behavior includes poly(N-isopropylacryamide) (PNIPAM). PNIPMA has its LCST close to the body temperature (32 °C). However, a concern has been raised on its toxicity due to the presence of residual monomers remaining in PNIPAM materials [53]. Alternative is poly(oligo(ethylene oxide) monomethyl ether methacrylate) (POEOMA) which has been known to be biocompatible and less immune response. Given its biocompatibility, the LCST of POEOMA could be adjusted by copolymerization of OEOMA with different EO lengths ranging at 25 – 90 °C [54, 55].

Table 1.1. Properties of polymers prepared with oligo(ethylene glycol) methacrylates of various length[53].

Polymer	Properties in aqueous environment	Commercial availability of the monomer
PMMA	Hydrophobic	Yes
PMEMA	Slightly hygroscopic	Yes
$PMEO_2MA$	LSCT ~ 26 °C	Yes
$PMEO_3MA$	LSCT ~ 52 °C	No
$POEGMA_{300}$	LSCT ~ 64 °C	Yes
$POEGMA_{475}$	LSCT ~ 90 °C	Yes

1.5 Scope of my master thesis

Conventional polyplex-based nanocarriers for nucleic-acid based therapy present critical drawbacks including cytotoxicity of cationic polymers, the degradation of nucleic acids in polyplexes, and the propensity to aggregate with serum proteins during blood circulation. Thus, we envisioned a strategy to avoid the drawbacks and limitations of current nucleic acid delivery nanocarriers which was designed based on complexes formed through ionic interactions between cationic copolymers and negatively charged nucleic acid therapeutics. As illustrated in Figure 1.7, the strategy centers on the design and synthesis of nucleic acids with functional groups that can act as both therapeutic and cross-linking agents. In contrast to polymerization approaches, therapeutic nucleic acids could be covalently bound to copolymers via reductive reactive degradable spacers as cross-links consisting of disulfide bonds. This approach could lead to the formation of nanogels covalently cross-linked with therapeutic nucleic acids. The reductive cleavage of the disulfide bond, in the presence of glutathione whose concentration is ≈ 10 mM within the cell, would trigger the separation of the therapeutic nucleic acid from the nanogel core. Therefore, this strategy would not require a proton-sponge effect.

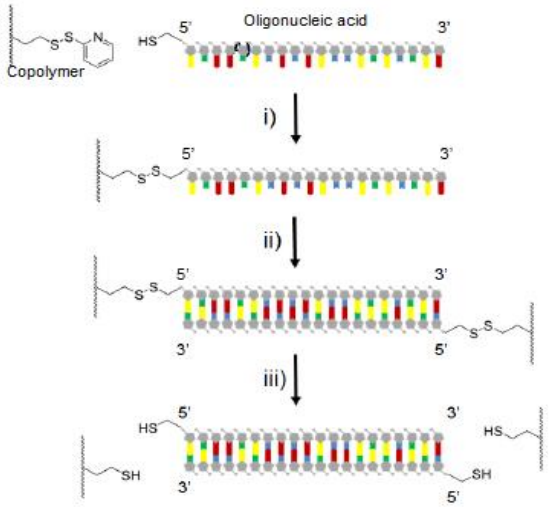

Figure 1.6. General approach for (i) conjugation of oligonucleotide to the copolymer, (ii) cross-linking between complementary oligonucleotides, (iii) glutathione triggered release of the duplex from the copolymer. Courtesy of Professors Oh and Wilds.

My MSc research has focused on the exploration of the strategy as a new paradigm for nucleic acid delivery in order to overcome the drawbacks of conventional polyplex-based delivery. A poly(phosphonic acid) terminated with thiol (SH) groups was synthesized by a combination of controlled radical polymerization, aminolysis, and hydrolysis as a mimic to a functional oligonucleotide. The formed homopolymer was covalently conjugated with a double hydrophilic, thermoresponsive random copolymer bearing pendant pyridyl-disulfide functional groups through a thiol-disulfide exchange reaction in aqueous solution. The formed nanogels crosslinked with disulfide bonds was characterized using analytical techniques such as dynamic light scattering and further they were examined for the reductive degradation upon the cleavage of disulfide linkages in the presence of glutathione (cellular reducing agent). Consequently, such reductive degradation of the fabricated nanogel could have the potential to prompt the detachment of therapeutic nucleic acids from the nanogel cores.

The first goal of my MSc project was to synthesize and characterize the poly(phosphonic acid) which serves as an oligonucleotide mimic, followed by quantification of terminal SH groups of the poly(phosphonic acid) by Ellman Assay. As illustrated in Figure 1.8, the second goal involves the synthesis and characterization of double hydrophilic random copolymer (called, PDSEMA-co-OEOMA), followed by evaluation of its thermoresponsive properties. The third goal is to explore the fabrication of nanogels from the reactive mixture of poly(phosphonic acid) with the random copolymer through thiol-disulfide exchange reaction as well as to study reductive degradation of the formed nanogels.

In the thesis, Chapter 2 contains an Experimental section, Chapter 3 the Results and Discussion, and Chapter 4 the Conclusion /Future works.

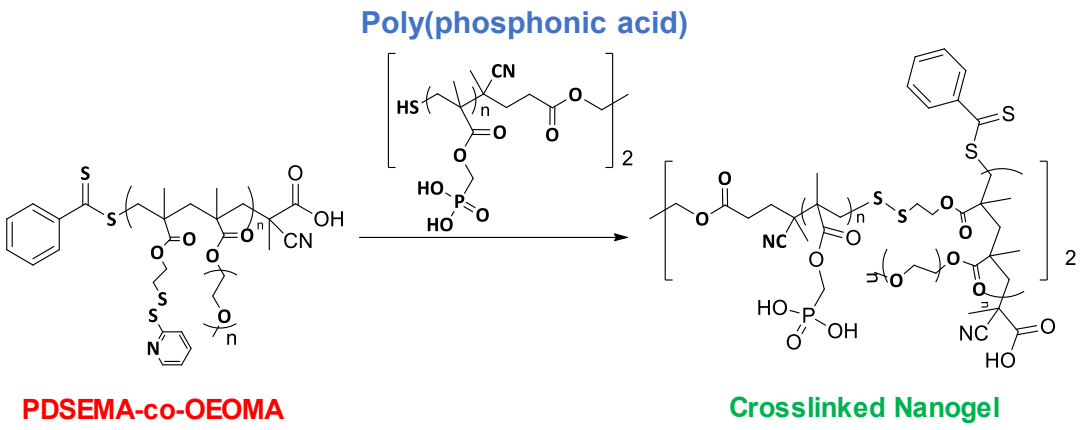

Figure 1.7. Synthetic scheme of a random copolymer as P(PDSEMA-co-OEOMA).

Chapter 2 Experimental

2.1 Instrumentation

^{1}H NMR spectra were recorded using a 500 MHz Varian spectrometer. The $CDCl_3$ singlet at 7.26 ppm and DMSO-d_6 quintet at 2.5ppm were selected as the reference standards. Molecular weight and molecular weight distribution were determined by gel permeation chromatography (GPC) equipped with a Viscotek VE1122 pump and a refractive index (RI) detector. One Plgel mixed-C column was used with THF at room temperature at a flow rate of 1.0 mL/min. Linear poly(methyl methacrylate) standards from Fluka were used for calibration. Aliquots of the polymer samples were dissolved in THF. The clear solutions were filtered using a 0.40 μm PTFE filter to remove any THF-insoluble species. A drop of anisole was added as a flow rate marker. Dynamic light scattering (DLS) was used to measure the size and size distribution of a block copolymer in aqueous solution at a fixed scattering angle of 175° at 25 °C, conducting with a Malvern Instruments Nano S ZEN1600 instrument equipped with a He-Ne laser operating at 633 nm. UV/vis spectra on an Agilent Cary 60 UV/vis spectrometer were recorded using a 1 cm wide quartz cuvette.

2.2 Materials

Methacryloyl chloride (MeCl, 97%), triethylamine (Et_3N, ≥99.5%), 2,2'-dithiodipyridine (Aldrithiol ^{TM}, 98%), 4-cyano-4-(phenylcarbonothioylthio)pentanoic acid (CPDA), N-(3-Dimethylaminopropyl)-N'-ethylcarbodiimide (EDC, ≥97%), azobisisobutyronitrile (AIBN), butylamine ($BuNH_2$, 98%), bromotrimethylsilane (TMSBr, 97%), ethylene glycol (EG, 99.8%), 5,5′-dithiobis(2-nitrobenzoic acid) (Ellman's agent, DTNB, 99%) were from Sigma-Aldrich and DL-dithiothreitol (DTT, 99%) from Acros Organics were purchased and used as received. Solvents

used include dichloromethane (DCM), dimethylformamide (DMF), tetrahydrofuran (THF), ethyl acetate (EA), hexane (H), and aqueous phosphate buffer solution at pH = 7.4 (PBS). Oligo(ethylene glycol) monomethyl ether methacrylate (OEOMA) with MW = 950 g/mol and EO units = 19 purchased from Aldrich was purified by passing through a column filled with basic alumina to remove inhibitors.

2.3 Synthesis of monomers and EG-RAFT

2.3.1. (Diethoxyphosphoryl)methyl methacrylate (DEPMMA)

An organic solution containing diethyl (hydroxymethyl)phosphonate (8.8mL, 59.5 mmol) and Et_3N (12.4mL, 89.2 mmol) dissolved in dried DCM (200 mL) was mixed with MeCl (13.7 mL, 65.4 mmol) in an ice-bath. The resulting mixture was stirred at room temperature for 24 hours. After the formed solids byproducts were removed by vacuum filtration, the solution was washed with an aqueous solution of sodium bicarbonate, dried with sodium sulfate, and then passed through a basic alumina column. The solvent was removed by a rotary evaporation and the product was dried in a vacuum oven at 70°C, yielding a colorless oil. Yield 12.04g (85.7%).

2.3.2. Pyridyldisulfide ethylmethacrylate (PDSEMA)

A solution containing HPDS (1.46 mL, 9 mmol) and Et_3N (1.25 mL, 10 mmol) dissolved in dry DCM (40 mL) was mixed with MeCl (1.36g, 10 mmol) dissolved in dry DCM (12 mL) in an ice-bath and the resulting mixture was kept under stirring for 6 hours at room temperature. The formed solids were removed by vacuum filtration and the product was washed with deionized water (30 mL) and brine solution (50 mL) twice. The organic layer was collected and dried over sodium sulfate. Solvent was removed by rotary evaporation to yield a yellow oil. The product was

purified by column chromatography with a mixture of ethyl acetate/hexane (1.5/8.5 v/v). The product was collected as the first of a total two bands from the silica gel column. Yield 0.79 g (64%).

2.3.3. A difunctional RAFT mediator (EG-RAFT)

An organic solution containing CPDA (50 mg, 0.18 mmol), EDC (34.3 mg, 0.18 mmol) and Et_3N (18 mg, 0.179 mmol) dissolved in anhydrous DCM (80 mL) was mixed with EG (3.7 mg, 0.0597mmol) dissolved in anhydrous DCM (20 mL) on an ice-bath for 30 min. The resulting mixture was kept at room temperature under stirring for 48 hours. After the removal of the solvents by rotary evaporation, the product was purified by silica gel column chromatography with a mixture of ethyl acetate/hexane (1/1 v/v) as an eluent. The product was collected as the first of a total two bands from the silica gel column. Yield 0.03 g (57%).

2.4 Synthesis of a telechelic polymer labeled with terminal thiols (B4-P3)

2.4.1. RAFT polymerization to synthesize B4-P1

DEPMMA (1.0 g, 4.23 mmol), EG-RAFT (24.8 mg, 0.042 mmol) and AIBN (3.3 mg, 0.017 mmol) dissolved in anisole were placed in a Schlenk flask and purged with nitrogen for 45 min. The resulting mixture was placed in an oil-bath preheated at 70 °C to start polymerization. After 5 hours, polymerization was stopped by cooling the Schlenk flask in an ice-bath and exposing it to air.

For purification, the crude product solution was precipitated from hexane to remove unreacted monomer and anisole. The precipitate was isolated and dried in a vacuum oven to yield B4-P1.

2.4.2. Aminolysis of P1 to synthesize B4-P2

The purified B4-P1 (0.9 g) in a nitrogen-purged THF (5 mL) was mixed with $BuNH_2$ (200 uL). The resulting mixture was stirred for 3 hours at room temperature until its red color turned to yellow. The products were then precipitated from a mixture of THF/hexane=1/25 v/v three times to remove excess $BuNH_2$ and cleaved phenylthiocarbonylthio species. Solvent was removed by rotary evaporation and the product was dried in a vacuum oven for 12 hours, yielding B4-P2.

2.4.3. Hydrolysis of P2 to synthesize B4-P3

The purified, dried B4-P2 (0.8 g) dissolved in anhydrous DCM (100 mL) was mixed with TMSBr (6 mL) under stirring for 3 hours at room temperature. Solvent was removed by rotary evaporation. The formed residues were mixed with MeOH for 1 hour at room temperature. Then, the solvent methanol was removed by rotary evaporation, and the concentrated solution was added dropwise to hexane to precipitate the polymer. The formed polymer was dissolved in MeOH. Then, the solvent was removed by rotary evaporation, and the formed polymer was dried in a vacuum oven at 40˚C for 12 hrs to yield B4-P3.

2.5 Ellman assay for quantitative analysis of thiols

2.5.1. Control experiment with DTT

Aqueous stock solutions were prepared with DTNB (2 mg) dissolved in PBS (1 mL) and DTT (1.5 mg) dissolved in PBS (2 mL). For Ellman assay, Ellman reagent solution (25 μL) and PBS (3 mL) were mixed with different volumes of DTT solution in test tubes. The resulting mixtures were incubated at room temperature for 15 min for UV/Vis spectroscopic analysis.

2.5.2. Experiments with B4-P3

Three aqueous solutions of DTNB (2 mg) dissolved in PBS (1 mL) were prepared and their UV/Vis spectra were recorded. The purified, dried B4-P3 of different amounts (2, 3, and 11 mg) were mixed with each solution and incubated at room temperature for 5 min. Their UV/vis spectra were recorded.

2.6 Synthesis of random copolymer (RP) by RAFT polymerization

PDSEMA (107.8 mg, 0.42 mmol), OEOMA (3610 mg, 3.8 mmol), EG-RAFT (11.8 mg, 0.042 mmol) and AIBN (2.4 mg, 13 mmol) were dissolved in anisole and purged with nitrogen for 45 mins. The resulting mixture was placed in an oil-bath preheated at 70 ℃ to start polymerization. After 7 hours, polymerization was stopped by cooling the Schlenk flask in an ice bath and exposing it to air.

For purification, the as-synthesized solution was precipitated from diethyl ether to remove unreacted monomers. The precipitates were collected and dried in a vacuum oven for 12 hours.

2.7 Thermoresponsiveness of PR in aqueous solution using DLS

The procedure described in the publication by the Dr. Oh's laboratory was followed [58]. Specially, aliquots of the dried PR (15 mg) were dissolved in deionized water (10 mL) to form clear aqueous solutions at a concentration of 1.5 mg/mL. The resulting solutions were filtered through 0.45 μm PES filters to remove large aggregates and dust. Their aliquots (1.2 mL) were transferred into a quartz cuvette, which were sealed with a Teflon stopper. The change in light

scattering intensity with temperature was then recorded from 20 to 90 °C at an increment of 1 °C. The LCST was determined from the onset of increase in light scattering intensity.

2.8 Fabrication of crosslinked nanogels

An aqueous solution of B4-P3 (3 mg) was dissolved in deionized water (40 mL) and its pH was adjusted to be pH = 7.5 by adding sodium bicarbonate. The resulting solution was mixed with an aqueous solution of RP (6.3 mg) dissolved in deionized water (40 mL). The mixture was heated to 60 °C overnight and allowed to cool down to room temperature to induce the thermoresponsive formation of nanogels.

2.9 Reductive-degradation of fabricated disulfide-crosslinked nanogels

Aliquots of the above nanogel dispersions were mixed with GSH (4 mg) under stirring for 1 day and DLS and UV/vis analysis were conducted to follow the reductive degradation.

Chapter 3 Results and Discussion

3.1 Synthesis of RAFT mediator and monomers

3.1.1. EG-CPDA RAFT mediator

As depicted in Figure 3.1a, EG-CPBA was synthesized by a facile carbodiimide coupling reaction with EDC for EG and CPBA at 1/3 mole ratio (equivalent to 2/3 mole equivalent of OH/COOH) in DCM at room temperature. The product was purified by column chromatography. ^{1}H NMR spectrum in Figure 3.1b shows the characteristic peaks at 4.3 ppm corresponding to the methylene protons adjacent to the ester bonds and peaks at 7.3-8.0 equivalent to aromatic protons. Their integrals are quantitative to the numbers of their protons, confirming the successful synthesis of EG-CPDA.

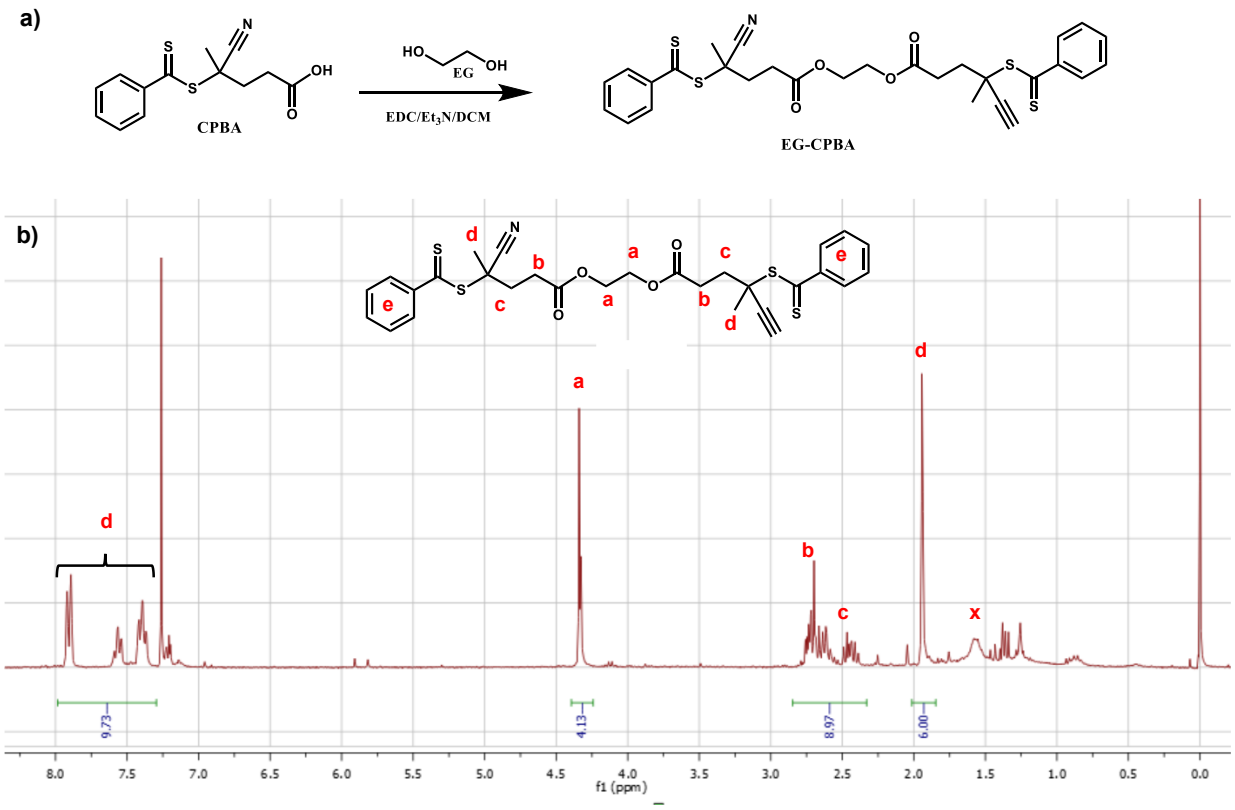

Figure 3.1. (a) Synthetic scheme and (b) ^{1}H NMR spectrum in $CDCl_3$ of EG-CPBA. Courtesy of Xiaolei Hu (a former MSc student in Dr. Oh's laboratory)

3.1.2. Methacrylate monomers

DEPMMA was synthesized by a reaction of MeCl with diethyl (hydroxymethyl)phosphonate in the presence of Et_3N as a base catalyst, as depicted in Figure 3.2a. ^1H NMR in Figure 3.2b shows the characteristic peaks and their integrals are quantitative, confirming the synthesis of DEPMMA.

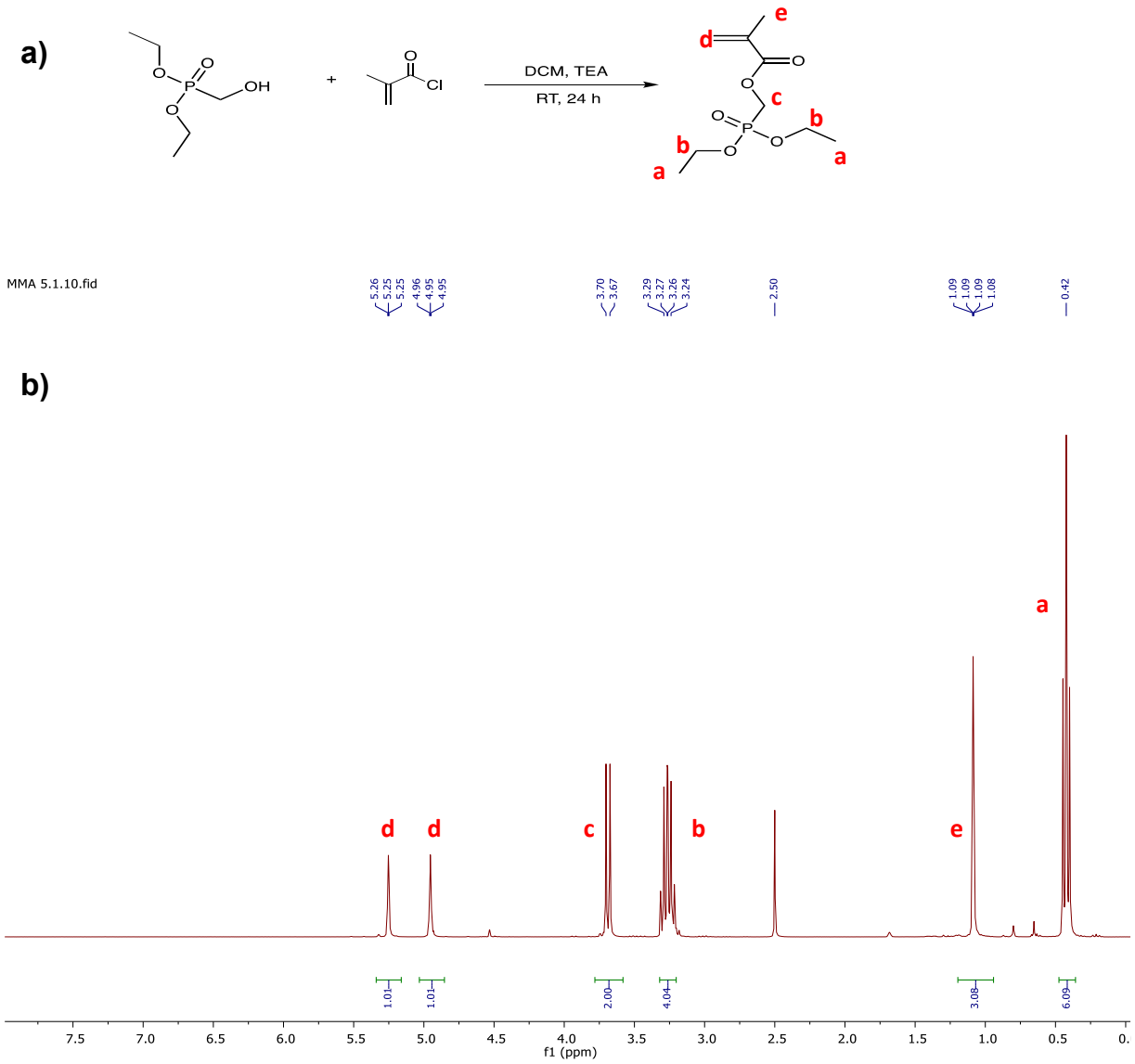

Figure 3.2. (a) Synthetic scheme and (b) ^1H NMR spectrum in DMSO-d_6 of DEPMMA. Courtesy of Dr. Nellepalli (a former postdoctoral fellow in Dr. Oh's laboratory).

PDSEMA was synthesized by two steps, as depicted in Figure 3.3a. The first step was the reaction of aldrithiol with mercaptoethanol in the presence of glacial acetic acid. After purification of the HPDS by column chromatography, the second step involved the reaction of the formed HPDS with MeCl in the presence of Et_3N. The ^1H NMR in Figure 3.3b-c confirms the synthesis of both HPDS precursor and PDSEMA.

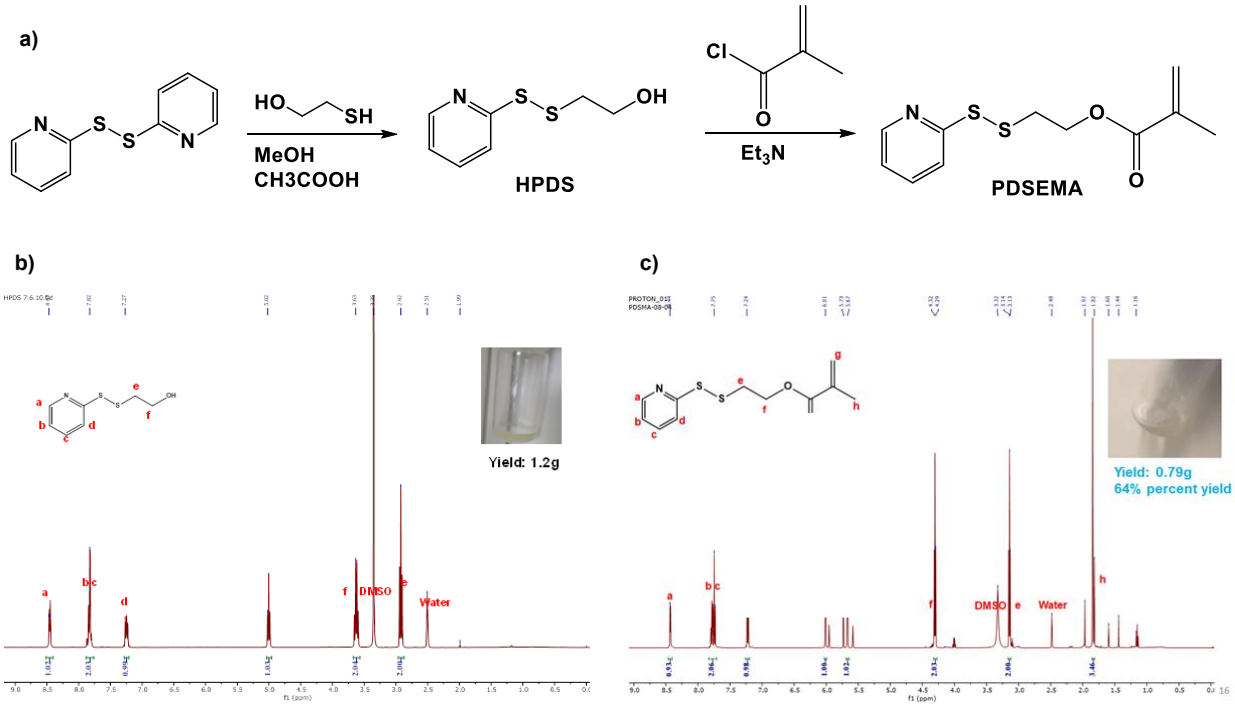

Figure 3.3. (a) Synthetic scheme and ^1H NMR spectra in DMSO-d_6 of (b) HPDS and (c) PDSEMA.

3.2 Synthesis of B4-P3

Figure 3.4 illustrates our approach to synthesize B4-P3 bearing terminal thiol groups, consisting of the synthesis of B4-P1, its aminolysis to B4-P2, and its hydrolysis to B4-P3.

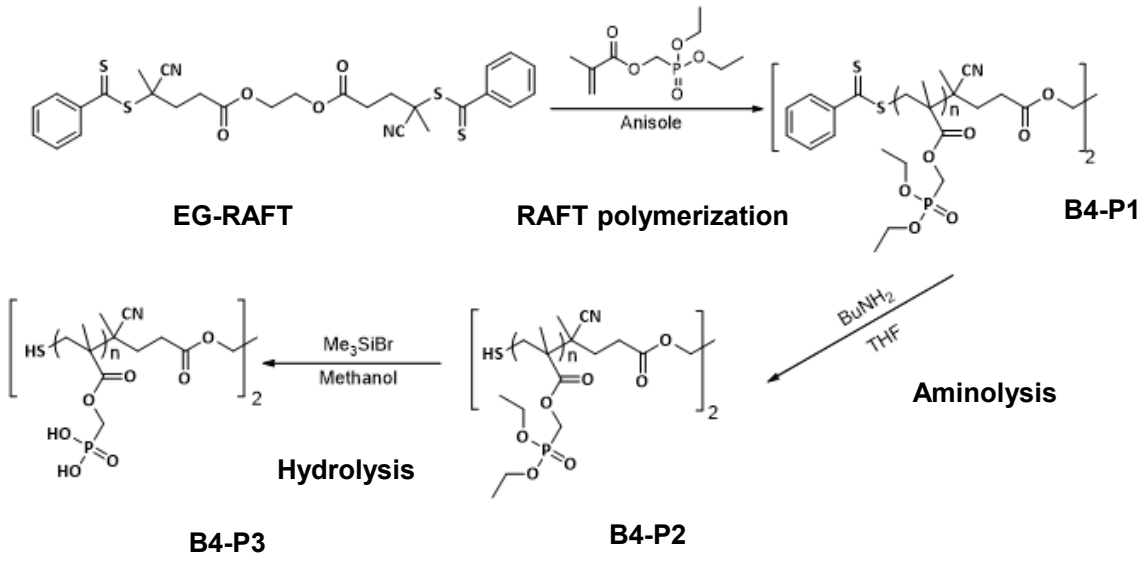

Figure 3.4. Reaction scheme for synthesis of telechelic poly(phosphonic acid) (PPA, B4-P3) with terminal thiol groups.

The first step involves the reversible addition fragmentation chain transfer (RAFT) polymerization for DEPMMA in the presence of EG-RAFT, initiated with AIBN, an azo initiator, in anisole solvent at 70 °C (Figure 3.5a). Under the initial mole ratio of $[DEPMMA]_0/[EG\text{-}RAFT]_0/[AIBN]_0 = 100/1/0.4$, the target degree of polymerization (DP) was set to be 100. The formed PEPMMA (B4-P1) was purified by precipitation from hexane and the composition of the purified polymer was determined using ^{1}H NMR spectroscopy. Figure 3.5b shows ^{1}H NMR spectrum of B4-P1. Peaks at 6.8 and 7.2 ppm correspond to aromatic protons in the RAFT moieties; the peaks at 4.35 ppm (C) and 4.12 ppm (b) correspond to the methylene protons adjacent to ester groups; the peak at 1.65 ppm (d) corresponds to the methyl groups in the phosphate group; and the peaks 1.2-0.7 ppm

correspond to the methyl group on PDEPMMA. Using the integrals of these peaks, the DP of DEPMMA unit was determined to be 28.

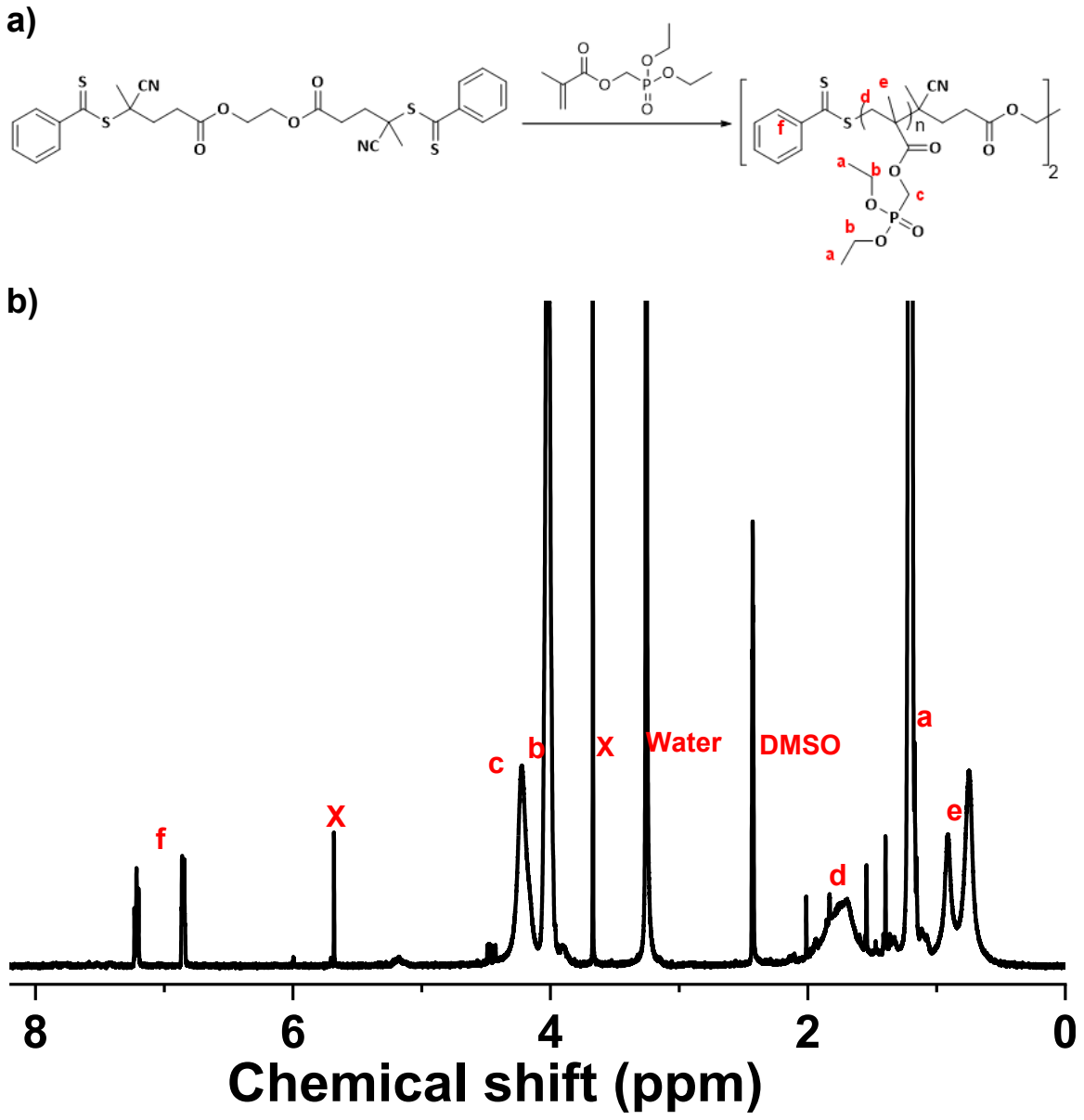

Figure 3.5. (a) Synthesis by RAFT polymerization and (b) ^{1}H NMR spectrum in DMSO-d_6 of B4-P1.

The second step is the aminolysis of the phenylthiocarbonylthiol terminal groups of B4-P1 in the presence of $BuNH_2$, as a typical amine catalyst in THF shown in Figure 3.6a. Figure 3.6b shows the ^1H NMR spectrum of B4-P2. The peaks at 6.8 and 7.2 ppm that correspond to aromatic protons in the RAFT moieties disappeared, confirming the removal of terminal phenylthiocarbonylthio groups.

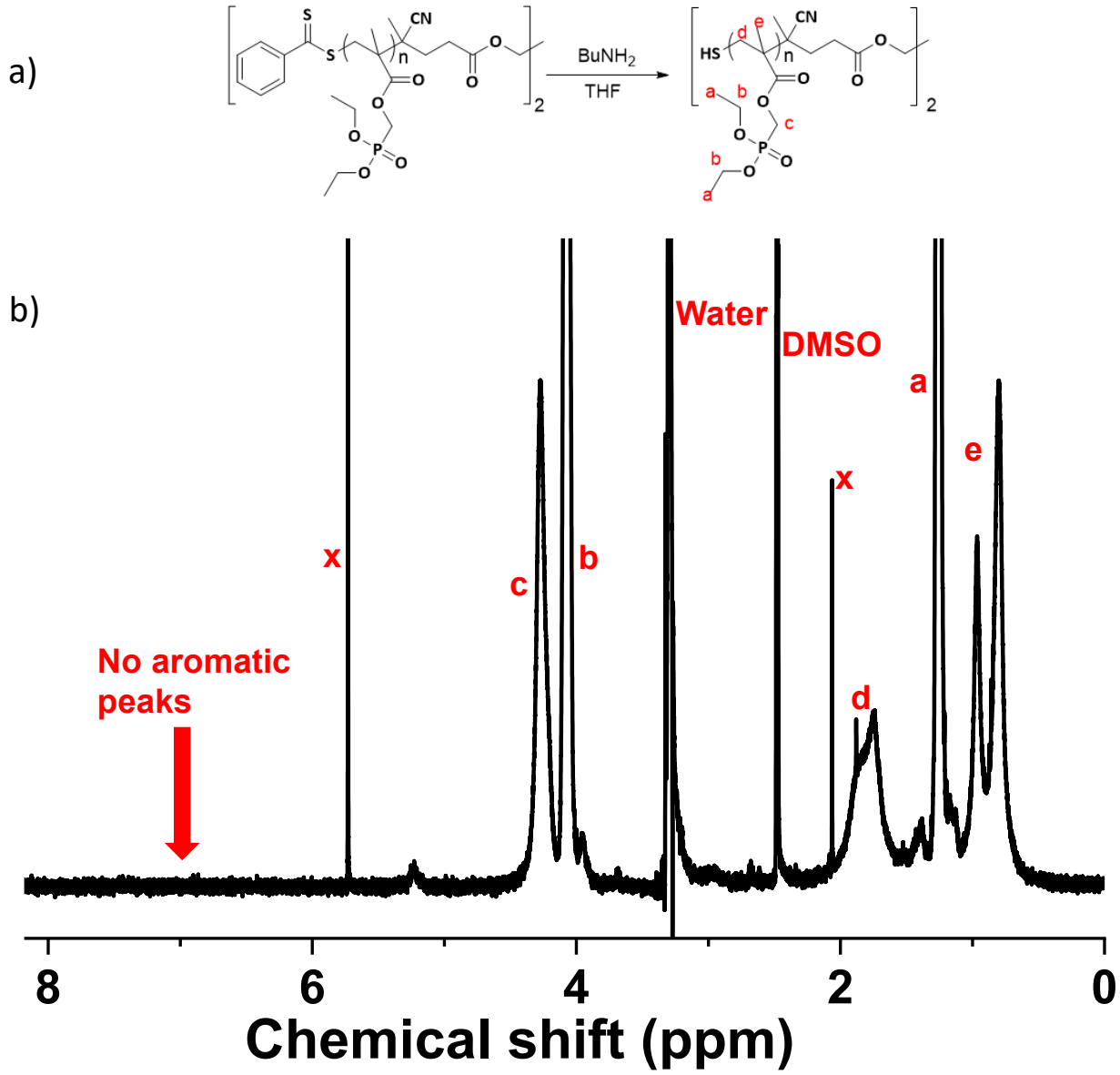

Figure 3.6. (a) Aminolysis of B4-P1 and (b) ^1H NMR spectrum of B4-P2 in DMSO-d_6.

Figure 3.7 shows the UV/vis spectrum of B4-P2, compared with B4-P1. The absorption at 305 nm [56] corresponding to the phenylthiocarbonylthio group completely disappeared after the treatment with $BuNH_2$. These results obtained from ^1H NMR and UV/vis spectroscopic analyses confirm the synthesis of B4-P2 through efficient aminolysis in the presence of a primary amine.

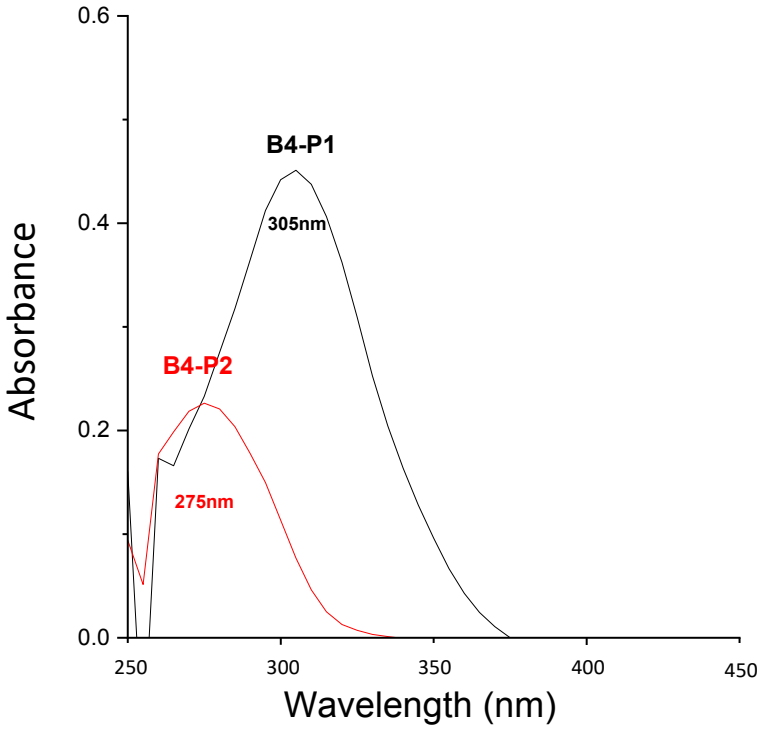

Figure 3.7. UV/Vis spectrum of B4-P2, compared with B4-P1 precursor in solvent, after aminolysis.

The last step is the hydrolysis of the pendant phosphate groups in B4-P2 in the presence of bromotrimethylsilane as an effectively selective reagent to the corresponding phosphoric acid groups. Figure 3.8 shows the ^1H NMR spectrum of B4-P3 in D_2O. The complete disappearance of the peak (c) can be expected upon the complete hydrolysis. Our ^1H-NMR analysis indicates that 88% of alkyl phosphonate groups were converted to phosphonic acid groups, meaning 12% of alkyl phosphonate groups remain in B4-P3.

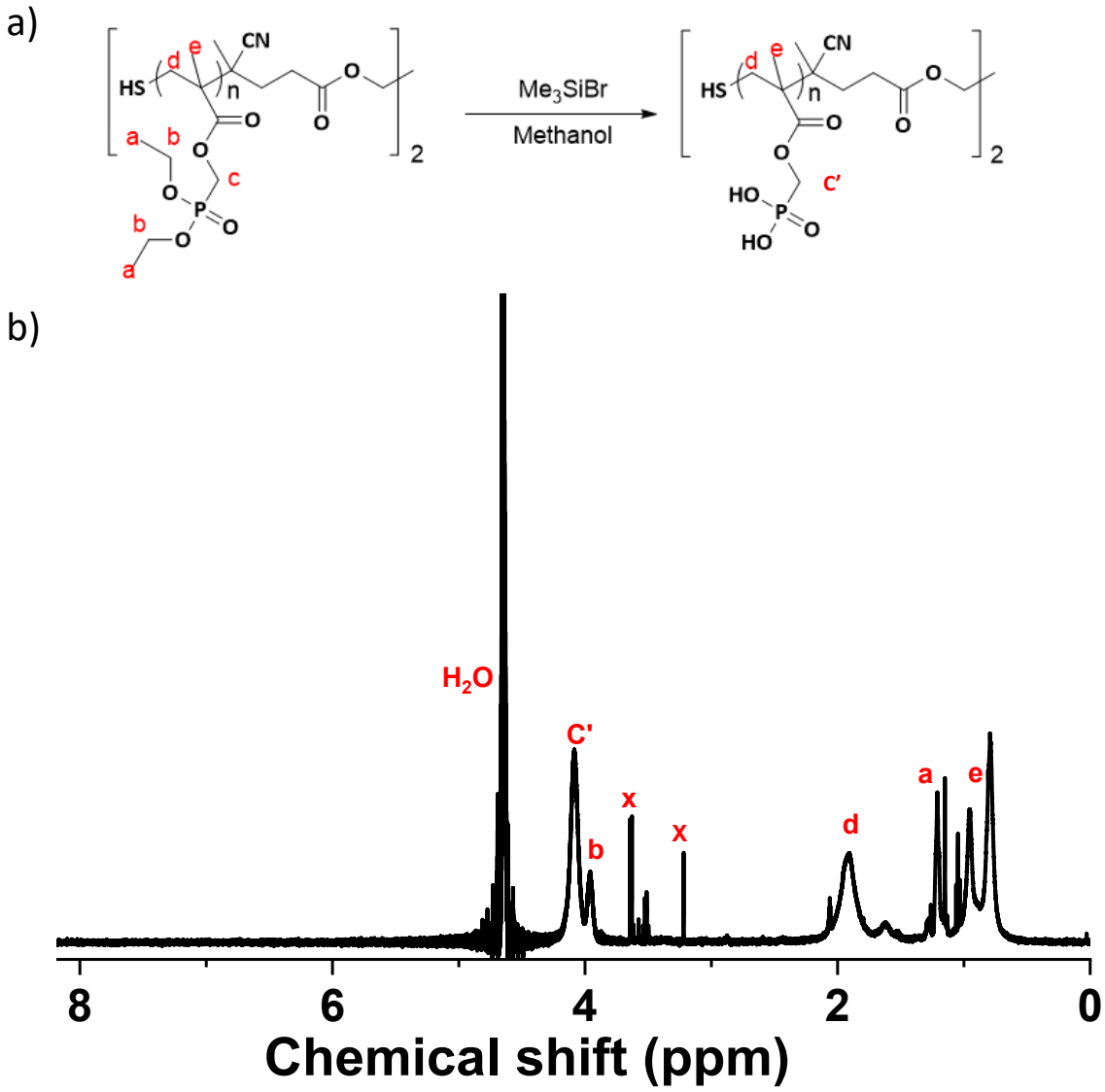

Figure 3.8. (a) Hydrolysis of B4-P2 and (b) ^{1}H NMR spectrum of B4-P3 in D_2O.

3.3 Analysis of terminal thiol groups in B4-P3

UV/Vis spectroscopy was used to qualitatively analyze the concentration of terminal thiol groups in B4-P3. As shown in Figure 3.9, a strong absorption at 265 nm corresponds to the terminal thiol groups in B4-P3. Although the absorption was blue shifted by 10 nm, compared to B4-P2 precursor (containing

phosphate pendants) in THF, such absorption confirms the terminal thiol groups are intact during hydrolysis.

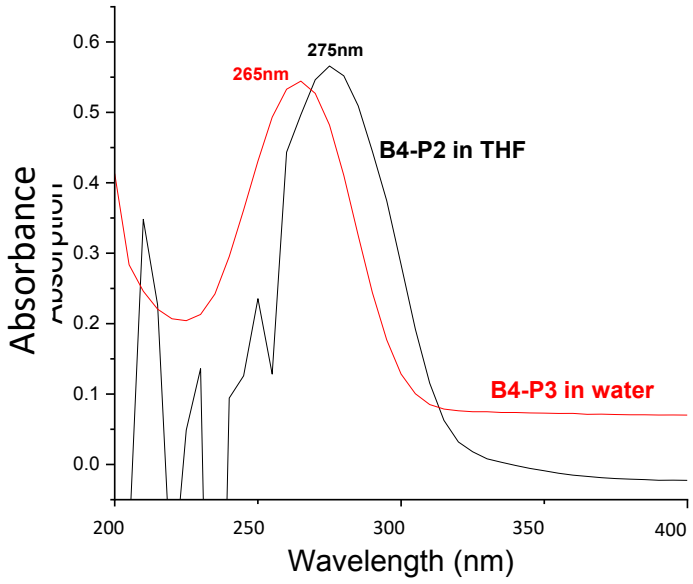

Figure 3.9. UV/Vis spectrum of B4-P3 in water, compared with B4-P2 in THF.

Further, the Ellman essay was performed in an attempt for the quantitative analysis of terminal thiol groups in B4-P3. In this assay, the DTNB having an aromatic disulfide bond is conjugated with a thiol through disulfide-thiol exchange reaction as shown in Figure 3-10. The generated NTB anion is UV-active and its absorbance at 412 nm can be used to determine the concentration of SH groups, along with the molar extinction coefficient of NTB ion which is 13,600 $M^{-1}cm^{-1}$ at 412 nm.

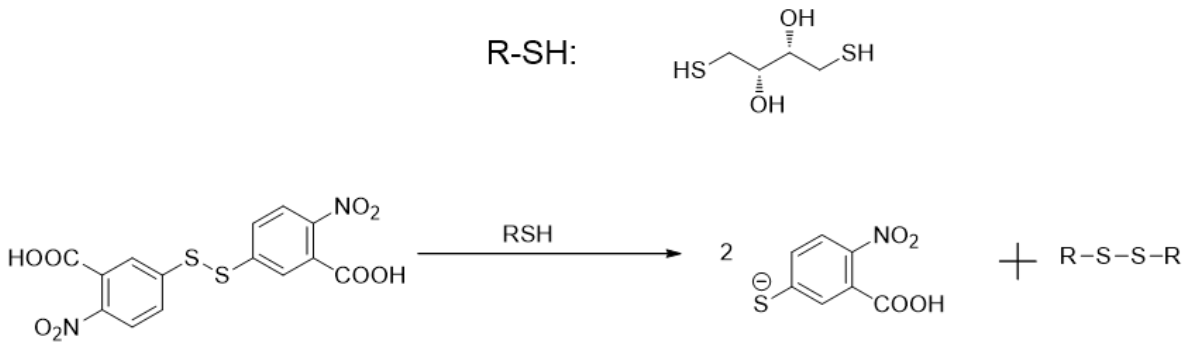

Figure 3.10. Schematic illustration of Ellman assay through the disulfide-thiol exchange reaction of DTNB with a thiol.

First, to get an insight into how the Ellman assay works and to determine the optimal concentration of thiols by the Ellman assay, a control experiment was conducted with DTT (a small molecule thiol) whose structure shown in Figure 3-8. The amount was varied as the mole ratio of DTT/DTNB to be 0.75/1, 1/1, and 1.4/1. Figure 3.11 shows the UV/Vis spectra of the three mixtures, compared with DTNB in water. DTNB had its absorption at 320 nm. When DTT was added, the absorption at 320 nm significantly decreased, while the absorption at 415 nm increased, confirming the occurrence of disulfide-thiol exchange, generating NTB ions.

Table 3.1 summarizes the characteristics and quantitative analysis with DTT. The trend observed revealed that when the amount of DTT is greater than 1 equivalent to DTNB, a reduced amount of thiol appeared to be detected by Ellman assay. Based on our results, 0.8/1-0.85/1 of thiol/DTNB could be optimal ratio for Ellman assay.

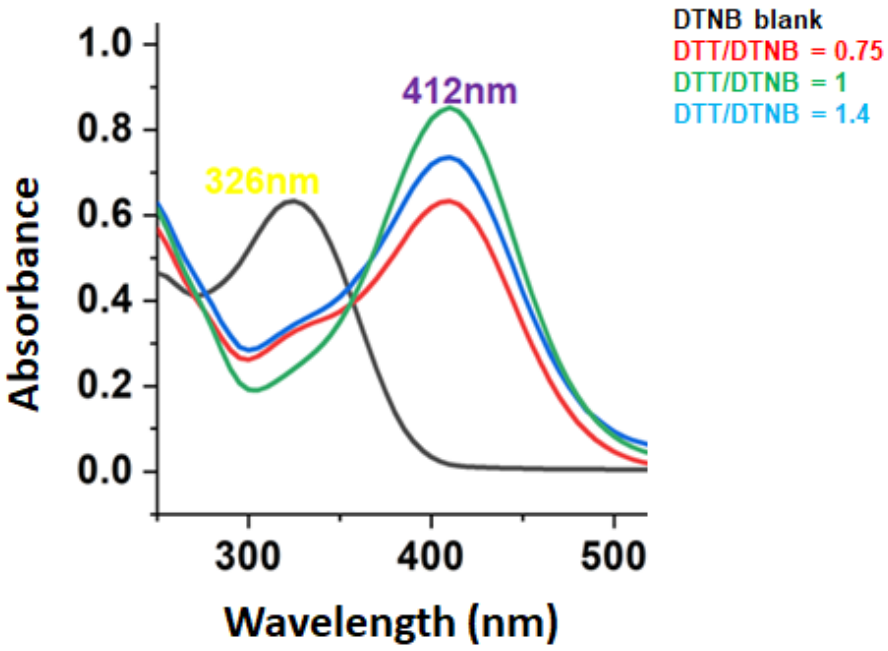

Figure 3.11. UV/Vis spectra of mixtures of DTNB with different amounts of DTT, compared with DTNB, in PBS.

Table 3.1. Characteristics and Quantitative analysis of thiol groups in DTT by Ellman assay using UV/vis spectroscopy.

DTT/DTNB mole ratio	0.75/1	1/1	1.4/1
DTT solution volume (μL)	25	35	45
DTT calculated in recipe (10^{-7} mol)	1.22	1.70	2.19
Absorbance at λ = 415 nm	0.612	0.714	0.829
DTT determined by Ellman assay (10^{-7} mol)	1.30	1.52	1.76
Deviation (%)	6	-10.9	-19.7

Next, the amount of thiol groups for B4-P3 was examined by the Ellman assay. Given the results with DTT, the mole equivalent ratio of DTNB/thiol group of 0.85/1 was initially chosen. However, no absorption at 415 nm was detected. The mole equivalent ratio (e.g. the amount of B4-P3) was increased up to 15/1. As seen in Figure 3.12, still no significant absorption at 412 nm was observed for the mixture of B4-P3 with DTNB. The reasons are not clear at this point, but plausibly it could be due to the nature

of terminal thiols groups attached to relatively long chains of B4-P3 polymer which makes the folded terminal thiol hard to interact with DTNB agent (see Table 3.2).

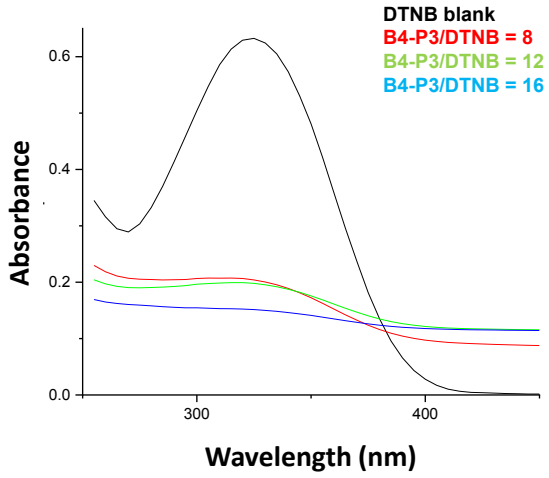

Figure 3.12. UV/Vis spectra of mixtures of DTNB with different amounts of B4-P3, compared with DTNB, in PBS.

Table 3.2. Characteristics and Quantitative analysis of Termina thiol group in B4-P4 by Ellman assay using UV/vis spectroscopy.

Mole equivalent of SH/DTNB	8/1	12/1	16/1
B4-P3 mass (mg)	8	11	15
SH mole equivalent (10^{-6} mol)	2.74	3.77	5.14
Absorbance at λ = 410 nm	0.084733	0.135288	0.177847
SH determined by Ellman assay (10^{-6} mol)	0.002	0.003	0.004

3.4 Synthesis of P(PDSEMA-co-OEOMA) random copolymer (RP)

As illustrated in Figure 3.13a, RAFT polymerization was employed for a mixture of PDSEMA and OEOMA at 9/1 mol ratio, in the presence of CPDA RAFT agent. The polymerization was initiated with AIBN, an azo initiator, in anisole solvent at 70 °C, under the initial mole ratio of $[OEOMA]_0/[PDSEMA]_0/[CPDA]_0/[AIBN]_0$ = 90/10/1/0.3 with the targeting DP = 100 at complete monomer conversion. Figure 3.13b shows the ^{1}H NMR spectrum of RP in DMSO-d_6. The peaks at 7.2-

8.5 ppm correspond to aromatic protons of pyridyl moieties in PDSEMA units. The peaks at 3.5 ppm correspond to OE protons in pendant OEO groups in OEOMA units and the peaks at 0.7-1.2 ppm correspond to the methyl groups on the backbones of both PDSEMA and OEOMA units. Using the integral ratios of these peaks, the mole% of PDSEMA units in the copolymer was determined to be 14% and the OEOMA units on copolymer was 86%.

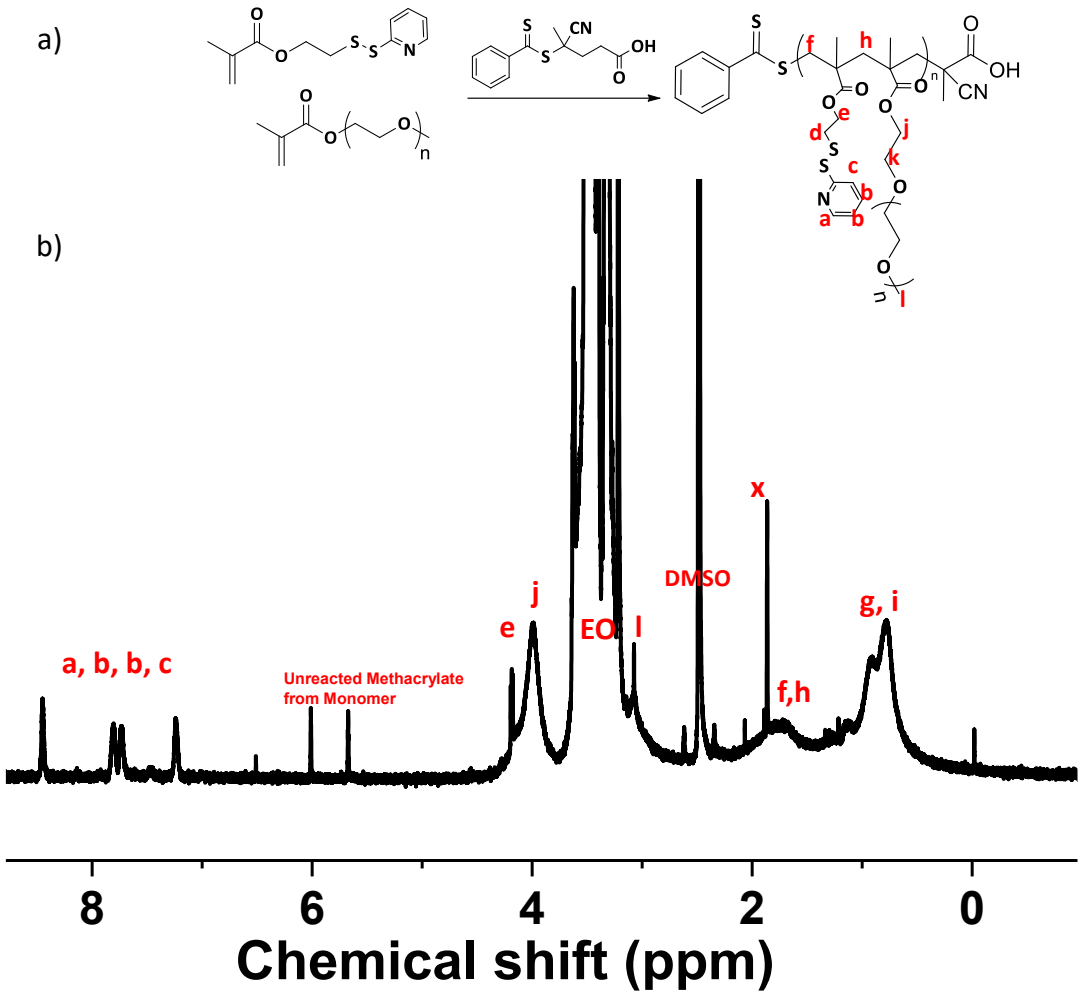

Figure 3.13. (a) Synthetic scheme and (b) ^{1}H NMR spectrum in DMSO-d_6 of RP random copolymer.

3.5 Investigation of thermoresponsive property of random copolymer

The synthesized random copolymer was examined for its thermoresponsiveness. The DLS technique was used to measure light scattering intensity or diameter of the RP over temperature in aqueous solution. Figure 3.14 shows the typical result as the evolution of diameter for a temperature ranging of 25 – 95 °C at 1.5 mg/mL. Because the diameters were scattered and did not show any trends, the results did not allow us to determine the lower critical solution temperature (called LCST) of RP in aqueous solution. Our further attempts with decreasing concentrations of RP ranging at 1.0-0.1 mg/mL did not appear to show its LCST as shown in Figure 3.15.

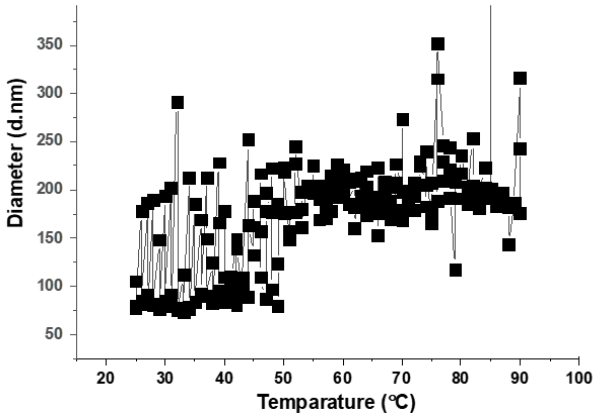

Figure 3.14. Typical example of evolution of diameter of RP in aqueous solution at concentration of 1.5mg/mL over temperature ranging at 25-90 °C in an attempt to determine its LCST.

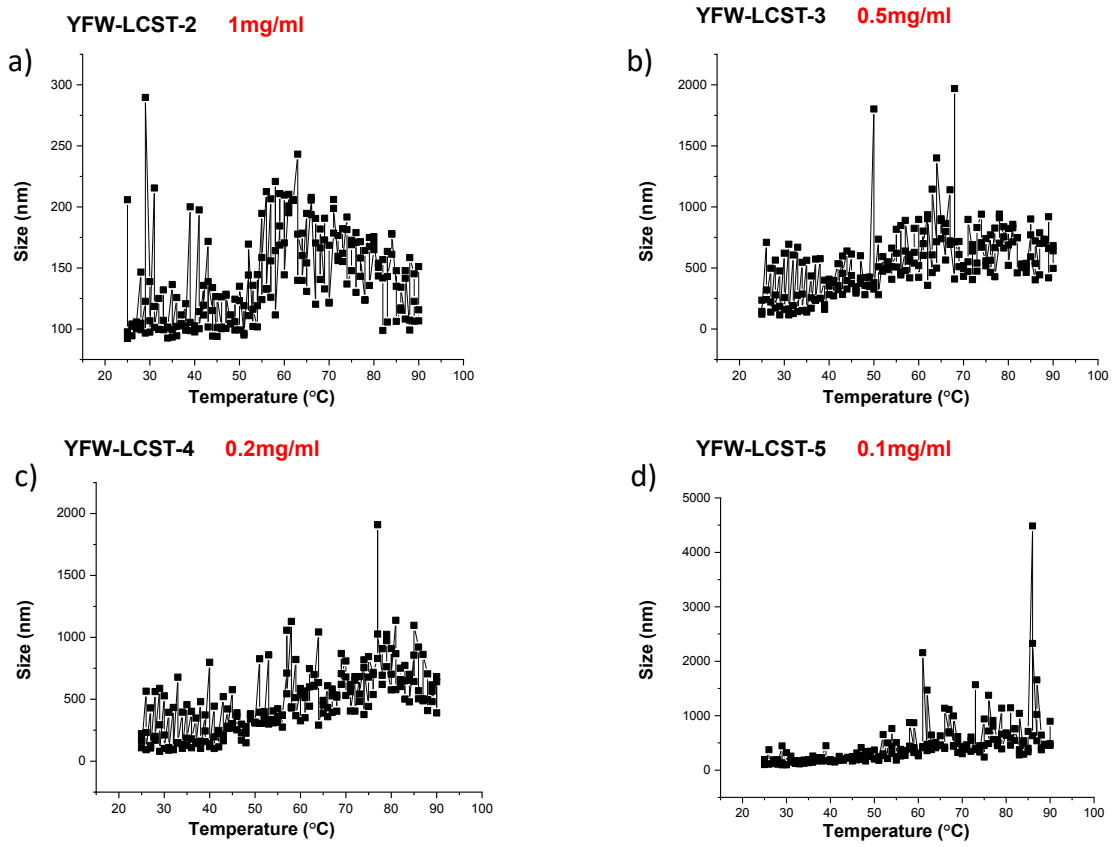

Figure 3.15. Evolution of diameter of RP in aqueous solution at the concentrations of (a) 1.0 mg/mL (b) 0.5 mg/mL (c) 0.2 mg/mL d) 0.1mg/mL over temperature ranging at 25-90 °C.

3.5 Fabrication of disulfide-crosslinked nanogels in water

The synthesized RP contains pyridyldisulfide pendants and B4-P3 is labeled with terminal thiol groups. As illustrated in Figure 3.16, the pendant pyridyldisulfide groups can react with the terminal thiol groups to form the corresponding disulfide bonds through thiol-disulfide exchange reactions, eliminating pyridine2-thiolate. Such reaction can be achieved for the mixture of RP with B4-P3 in water, yielding disulfide-crosslinked polymers in the form of nanometer-sized hydrogel (called nanogel).

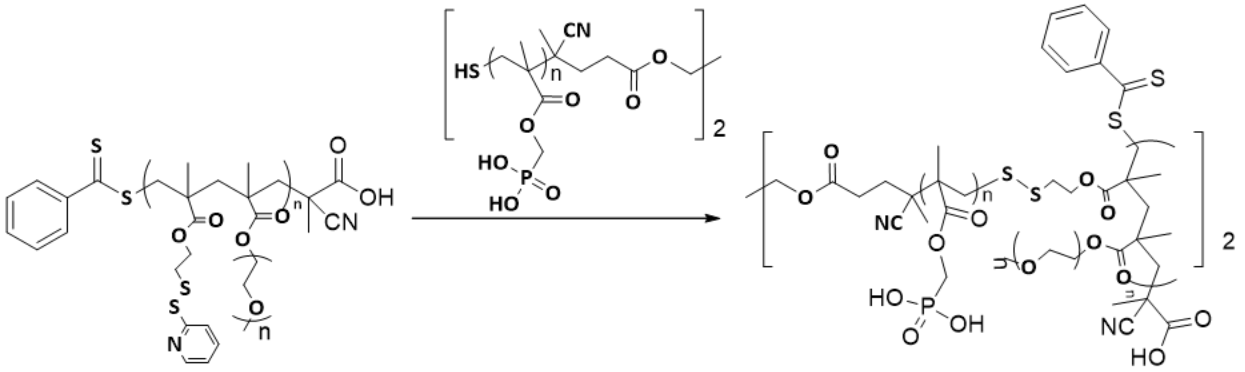

Figure 3.16. Scheme to illustrate the fabrication of disulfide-labeled reduction-degradable nanogels through the disulfide-thiol exchange reaction of RP having pyridyldisulfide pendants with B4-P3 having terminal thiol groups in water.

A challenge for the procedure is that the optimal concentration of RP and B4-P3 in water must be found in order to avoid the formation of large aggregates or even standing gel. Thus, their concentrations were varied from 0.002 – 0.12 mg/mL as the mole equivalent ratio of pyridyldisulfide (in RP)/thiol (B4-P3) = 1/1 was kept. DLS was used to follow the formation of nanogels. Figure 3-17 shows the size distribution of random copolymer over different parameters such as various concentration of aqueous solution, participation of catalyst and pH value. The result from DLS measurement over the various parameters cannot confirm the formation of nanogel, therefore reductive degradation was attempted.

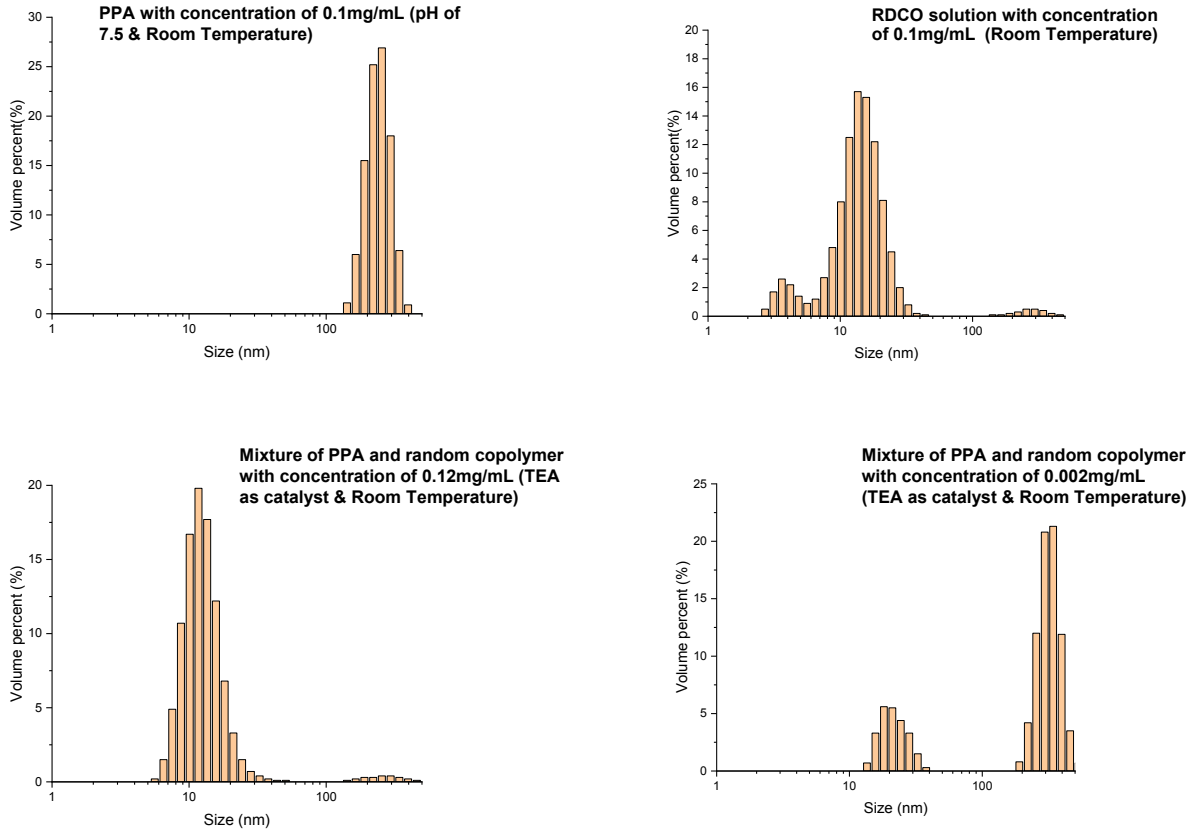

Figure 3.17. Evolution of size distribution of RP in aqueous solution over different parameters

3.6 Reductive degradation of disulfide-crosslinked nanogels

The formed nanogels containing disulfide bonds should undergo degradation in the presence of glutathione (GSH) through thiol-disulfide exchange reactions. As a preliminary examination of such a response by GSH, the formed nanogels were incubated with excess GSH in water and DLS was used to follow any changes of the nanogels.

UV spectrum of the mixture of RP with B4-P3 in water shows no significant absorption at 280 nn, which corresponds to the absorption of RP and B4-P3. However, it exhibits a small absorption at 300 – 320 nm, which appears to be characteristic for a disulfide bond. These results could suggest the possible occurrence of thiol-disulfide exchange reactions of pyridyldisulfide pendants of RP with

terminal thiols of B4-P3, resulting in the formation of crosslinked polymers in water. However, no absorption at 343 nm was observed which corresponds to pyridothione that can be generated from pyridyldisulfide groups as byproduct at 343 nm [57]. GSH can react with a disulfide-containing compound and therefore detach the cross-linked nanogel. After adding GSH to the aqueous solution, a shift in the peak of the mixture is observed in the UV spectrum as shown on Figure 3.18.

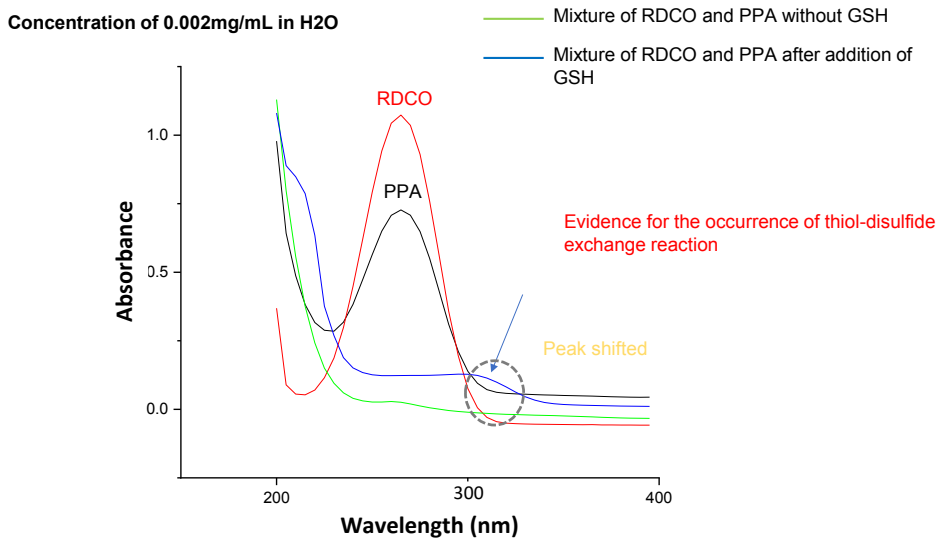

Figure 3.18. UV/Vis spectrum of a mixture of RP+B4-P3, compared with individuals of RP and B4-P3, in water, mixture before and after addition of GSH.

The DLS technique was examined to follow any change in average size and size distribution of the nanogels upon the addition of GSH. Figure 3.19 shows the slight increase in their average diameter from 595nm to 576nm, which might indicate the degradation of nanogels to some degree.

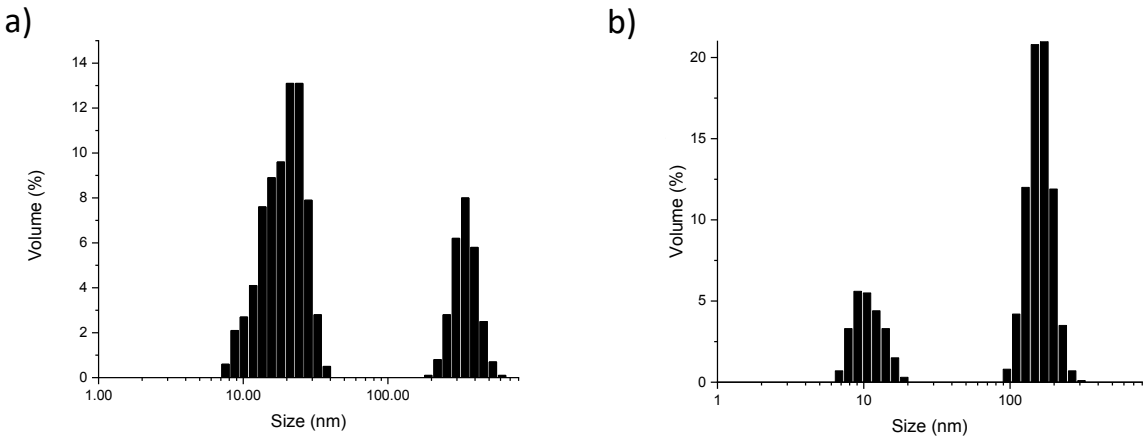

Figure 3.19. Comparison of size distribution (a) before and (b) after addition of GSH by DLS measurement.

Chapter 4 Conclusion and Future Work

EG-RAFT agent was synthesized by a facile coupling reaction of CPDA RAFT agent with EG. The RAFT polymerization for DEPMMA in the presence of EG-RAFT generated B4-P1. Aminolysis and hydrolysis was proceeded with B4-P1 to generate poly-phosphonic acid B4-P3 bearing terminal thiol groups with > 88% conversion. UV/vis spectroscopy was used to qualitatively analyze the presence of terminal thiol groups in B4-P3 and the absorption at 265 nm in the spectrum confirms the terminal thiol groups are intact during hydrolysis. Further, the Ellman essay was performed in an attempt for the quantitative analysis of terminal thiol groups in B4-P3. Unfortunately, the detected quantity of NTB anion does not increase proportionally with the increase in the amount of polymer due to the nature of terminal thiols groups attached to relatively long chains of B4-P3 polymer. RAFT polymerization was employed for a mixture of PDSEMA and OEOMA at 9/1 mol/mol ratio to synthesize P(DSEMA-co-OEOMA) with 14 mol% of PDSEMA units and 86 mol% OEOMA units. The synthesized random copolymer was examined for its thermoresponsiveness utilizing DLS. However, the lower critical solution temperature (called LCST) of RP cannot be determined as the diameters were scattered and did not show any trends.

Theoretically, RP polymer bearing pendant pyridyldisulfide groups can react with the terminal thiol groups from B4-P3 to form the corresponding disulfide bonds through thiol-disulfide exchange reactions yielding disulfide-crosslinked polymers in the form of nanogel. The result form DLS measurement over various parameters could not confirm the formation of nanogels. The reductive degradation experiment was performed as the nanogels containing disulfide bonds could be degraded in the presence of GSH through thiol-disulfide exchange reactions, UV/vis and DLS detected the change before and after the addition of GSH. Based on the UV-vis spectrum, the by-product pyridothione that was generated from pyridyldisulfide was not observed at 343 nm, and the peak representing the mixture

is shifted after the addition of GSH. The result from DLS measurement gave another clue for the occurence of degradation of cross-linked nanogel as the particle size distribution shifted.

Future work consists of i) further characterization of cross-linked nanogel in aqueous solution as well as the corresponding reductive degradation of nanogel over different parameters such as pH, concentration or catalyst; ii) the experiments exploring the conjugation of P(DSEMA-co-OEOMA) with the oligonucleotides with terminal SH groups, and the reductive degradation of that carrier and finally iii) in vivo experiments of nanogels that are carriers of oligonucleotides.

References

[1] Wolf, George. "Friedrich Miescher, the man who discovered DNA." *Chemical Heritage* 21.10-11 (2003): 37-41.

[2] Dahm, Ralf. "Discovering DNA: Friedrich Miescher and the early years of nucleic acid research." *Human genetics* 122 (2008): 565-581.

[3] Watson, James D., and Francis HC Crick. "The Complementary Structure of Deoxyribonucleic Acid." *Nature* 171 (1953): 737-738.

[4] Wolf, George. "Friedrich Miescher, the man who discovered DNA." *Chemical Heritage* 21.10-11 (2003): 37-41.

[5] Travers, Andrew, and Georgi Muskhelishvili. "DNA structure and function." *The FEBS journal* 282.12 (2015): 2279-2295.

[6] Chargaff, Erwin, et al. "The composition of the desoxyribonucleic acid of salmon sperm." *Journal of Biological Chemistry* 192.1 (1951): 223-230.

[7] Minchin, Steve, and Julia Lodge. "Understanding biochemistry: structure and function of nucleic acids." *Essays in biochemistry* 63.4 (2019): 433-456.

[8] Kulkarni, Jayesh A., et al. "The current landscape of nucleic acid therapeutics." *Nature nanotechnology* 16.6 (2021): 630-643.

[9] Opalinska, Joanna B., and Alan M. Gewirtz. "Nucleic-acid therapeutics: basic principles and recent applications." *Nature Reviews Drug Discovery* 1.7 (2002): 503-514.

[10] Bost, Jeremy P., et al. "Delivery of oligonucleotide therapeutics: Chemical modifications, lipid nanoparticles, and extracellular vesicles." *ACS nano* 15.9 (2021): 13993-14021.

[11] Gupta, Akash, et al. "Nucleic acid delivery for therapeutic applications." *Advanced Drug Delivery Reviews* 178 (2021): 113834.

[12] Dorsett, Yair, and Thomas Tuschl. "siRNAs: applications in functional genomics and potential as therapeutics." *Nature reviews Drug discovery* 3.4 (2004): 318-329.

[13] Egli, Martin, and Muthiah Manoharan. "Chemistry, structure and function of approved oligonucleotide therapeutics." *Nucleic Acids Research* 51.6 (2023): 2529-2573.

[14] Dias, Nathalie, and C. A. Stein. "Antisense oligonucleotides: basic concepts and mechanisms." *Molecular cancer therapeutics* 1.5 (2002): 347-355.

[15] Pai, Sara Isabel, et al. "Prospects of RNA interference therapy for cancer." *Gene therapy* 13.6 (2006): 464-477.

[16] Dong, Yizhou, Daniel J. Siegwart, and Daniel G. Anderson. "Strategies, design, and chemistry

in siRNA delivery systems." *Advanced drug delivery reviews* 144 (2019): 133-147.

[17] Mintzer, Meredith A., and Eric E. Simanek. "Nonviral vectors for gene delivery." *Chemical reviews* 109.2 (2009): 259-302.

[18] Adler, Andrew F., and Kam W. Leong. "Emerging links between surface nanotechnology and endocytosis: impact on nonviral gene delivery." *Nano today* 5.6 (2010): 553-569.

[19] Jovic, Marko, et al. "The early endosome: a busy sorting station for proteins at the crossroads." *Histology and histopathology* 25.1 (2010): 99.

[20] Miyata, Kanjiro, Nobuhiro Nishiyama, and Kazunori Kataoka. "Rational design of smart supramolecular assemblies for gene delivery: chemical challenges in the creation of artificial viruses." *Chemical Society Reviews* 41.7 (2012): 2562-2574.

[21] Miyata, Kanjiro, R. James Christie, and Kazunori Kataoka. "Polymeric micelles for nano-scale drug delivery." *Reactive and Functional Polymers* 71.3 (2011): 227-234.

[22] Garnet, M. C. "Gene-delivery systems using cationic polymer." *Crit Rev Ther Drug Carrier Syt* 16 (1999): 147-207.

[23] Hwang, S. J., and M. E. Davis. "Cationic polymers for gene delivery: designs for overcoming barriers to systemic administration." *Current opinion in molecular therapeutics* 3.2 (2001): 183-

191.

[24] Sun, Xiaoli, and Na Zhang. "Cationic polymer optimization for efficient gene delivery." *Mini reviews in medicinal chemistry* 10.2 (2010): 108-125.

[25] Zhang, Shubiao, et al. "Cationic compounds used in lipoplexes and polyplexes for gene delivery." *Journal of controlled release* 100.2 (2004): 165-180.

[26] Farrell, Laura-Lee, et al. "A comparison of the effectiveness of cationic polymers poly-L-lysine (PLL) and polyethylenimine (PEI) for non-viral delivery of plasmid DNA to bone marrow stromal cells (BMSC)." *European journal of pharmaceutics and biopharmaceutics* 65.3 (2007): 388-397.

[27] Boussif, Otmane, et al. "A versatile vector for gene and oligonucleotide transfer into cells in culture and in vivo: polyethylenimine." *Proceedings of the National Academy of Sciences* 92.16 (1995): 7297-7301.

[28] Song, Hongmei, et al. "Cationic lipid-coated PEI/DNA polyplexes with improved efficiency and reduced cytotoxicity for gene delivery into mesenchymal stem cells." *International journal of nanomedicine* (2012): 4637-4648.

[29] Agarwal, Seema, et al. "PDMAEMA based gene delivery materials." *Materials Today* 15.9 (2012): 388-393.

[30] Samsonova, Olga, et al. "Low molecular weight pDMAEMA-block-pHEMA block-copolymers synthesized via RAFT-polymerization: potential non-viral gene delivery agents." *Polymers* 3.2 (2011): 693-718.

[31] Kunath, Klaus, et al. "Low-molecular-weight polyethylenimine as a non-viral vector for DNA delivery: comparison of physicochemical properties, transfection efficiency and in vivo distribution with high-molecular-weight polyethylenimine." *Journal of Controlled Release* 89.1 (2003): 113-125.

[32] de Ilarduya, Conchita Tros, Yan Sun, and Nejat Düzgüneş. "Gene delivery by lipoplexes and polyplexes." *European journal of pharmaceutical sciences* 40.3 (2010): 159-170.

[33] Akagi, D., et al. "Biocompatible micellar nanovectors achieve efficient gene transfer to vascular lesions without cytotoxicity and thrombus formation." *Gene therapy* 14.13 (2007): 1029-1038.

[34] Wei, Hua, Ren-Xi Zhuo, and Xian-Zheng Zhang. "Design and development of polymeric micelles with cleavable links for intracellular drug delivery." *Progress in polymer Science* 38.3-4 (2013): 503-535.

[35] Rijcken, C. J. F., et al. "Triggered destabilisation of polymeric micelles and vesicles by changing polymers polarity: an attractive tool for drug delivery." *Journal of controlled*

release 120.3 (2007): 131-148.

[36] Alvarez-Lorenzo, Carmen, and Angel Concheiro. "Smart drug delivery systems: from fundamentals to the clinic." *Chemical communications* 50.58 (2014): 7743-7765.

[37] Loomis, Kristin, Kathleen McNeeley, and Ravi V. Bellamkonda. "Nanoparticles with targeting, triggered release, and imaging functionality for cancer applications." *Soft Matter* 7.3 (2011): 839-856.

[38] Mura, Simona, Julien Nicolas, and Patrick Couvreur. "Stimuli-responsive nanocarriers for drug delivery." *Nature materials* 12.11 (2013): 991-1003.

[39] Delplace, Vianney, and Julien Nicolas. "Degradable vinyl polymers for biomedical applications." *Nature chemistry* 7.10 (2015): 771-784.

[40] Zhang, Qian, Na Re Ko, and Jung Kwon Oh. "Recent advances in stimuli-responsive degradable block copolymer micelles: synthesis and controlled drug delivery applications." *Chemical communications* 48.61 (2012): 7542-7552.

[41] Bawa, Kamaljeet K., and Jung Kwon Oh. "Stimulus-responsive degradable polylactide-based block copolymer nanoassemblies for controlled/enhanced drug delivery." *Molecular pharmaceutics* 14.8 (2017): 2460-2474.

[42] Jazani, Arman Moini, and Jung Kwon Oh. "Development and disassembly of single and multiple acid-cleavable block copolymer nanoassemblies for drug delivery." *Polymer Chemistry* 11.17 (2020): 2934-2954.

[43] Cheng, Ru, et al. "Glutathione-responsive nano-vehicles as a promising platform for targeted intracellular drug and gene delivery." *Journal of controlled release* 152.1 (2011): 2-12.

[44] Russo, Angelo, et al. "Selective modulation of glutathione levels in human normal versus tumor cells and subsequent differential response to chemotherapy drugs." *Cancer research* 46.6 (1986): 2845-2848.

[45] Ko, Na Re, et al. "Reductively-sheddable cationic nanocarriers for dual chemotherapy and gene therapy with enhanced release." *Colloids and Surfaces B: Biointerfaces* 126 (2015): 178-187.

[46] Shetty, Chaitra, et al. "Dual-location dual-acid/glutathione-degradable cationic micelleplexes through hydrophobic modification for enhanced gene silencing." *Molecular Pharmaceutics* 17.10 (2020): 3979-3989.

[47] Barker, J. A., and W. Fock. "Theory of upper and lower critical solution temperatures." *Discussions of the Faraday Society* 15 (1953): 188-195.

[48] Zhang, Qilu, et al. "Thermoresponsive polymers with lower critical solution temperature: from fundamental aspects and measuring techniques to recommended turbidimetry

conditions." *Materials Horizons* 4.2 (2017): 109-116.

[49] Saeki, Susumu, et al. "Upper and lower critical solution temperatures in poly (ethylene glycol) solutions." *Polymer* 17.8 (1976): 685-689.

[50] Pasparakis, George, and Constantinos Tsitsilianis. "LCST polymers: Thermoresponsive nanostructured assemblies towards bioapplications." *Polymer* 211 (2020): 123146.

[51] Hogan, Katie J., and Antonios G. Mikos. "Biodegradable thermoresponsive polymers: Applications in drug delivery and tissue engineering." *Polymer* 211 (2020): 123063.

[52] Yan, Lesan, and Xingde Li. "Biodegradable stimuli-responsive polymeric micelles for treatment of malignancy." *Current pharmaceutical biotechnology* 17.3 (2016): 227-236.

[53] Lutz, Jean-François. "Polymerization of oligo (ethylene glycol)(meth) acrylates: Toward new generations of smart biocompatible materials." *Journal of Polymer Science Part A: Polymer Chemistry* 46.11 (2008): 3459-3470.

[54] Wang, X-S., et al. "Facile synthesis of well-defined water-soluble polymers via atom transfer radical polymerization in aqueous media at ambient temperature." *Chemical Communications* 18 (1999): 1817-1818.

[55] Coullerez, Géraldine, et al. "Understanding copper-based atom-transfer radical

polymerization in aqueous media." *The Journal of Physical Chemistry A* 108.35 (2004): 7129-7131.

[56] Ryu, Ja-Hyoung, et al. "Self-cross-linked polymer nanogels: a versatile nanoscopic drug delivery platform." *Journal of the American Chemical Society* 132.48 (2010): 17227-17235.

[57] Wu, Peidong, et al. "Influence of Polymer Structure and Architecture on Drug Loading and Redox-Triggered Release." *Biomacromolecules* 23.1 (2021): 339-348.

[58] Chan, Nicky, et al. "Dual Redox and Thermoresponsive Double Hydrophilic Block Copolymers with Tunable Thermoresponsive Properties and Self-Assembly Behavior." *Macromolecular rapid communications* 35.7 (2014): 752-757.